united nations educational, scientific and cultural organization

international atomic energy agency

the
abdus salam
international centre for theoretical physics

SMR/1325-9

Workshop on

Nuclear Data for Science & Technology: Accelerator Driven Waste Incineration

10 - 21 September 2001

Miramare - Trieste, Italy

Monte Carlo simulations of nuclear experiments - code FLUKA

P.R. Sala
CERN, Geneva, Switzerland

Monte Carlo simulations of nuclear experiments - code FLUKA

Workshop on .. Nuclear Data for Science & Technology: Accelerator Driven Waste Incineration

ICTP Trieste 17-21 Sept. 2001

P.R Sala[2]

[2] CERN (on leave from INFN-Milan)

FLUKA

Authors: **A. Fassò[†], A. Ferrari[&], J. Ranft[*], P.R. Sala[&]**
[†] **CERN,** [&] **INFN Milan and CERN,** [*] **Siegen University**

Interaction and transport MonteCarlo code

- Hadron-hadron and hadron-nucleus interactions 0-100 TeV
- Nucleus-nucleus interactions 0-10000 TeV/n: *under development*
- Electromagnetic and μ interactions 1 keV-100 TeV
- Neutrino interactions
- Charged particle transport including all relevant processes
- Transport in magnetic field
- Combinatorial (boolean) geometry
- Neutron multigroup transport and interactions 0-20 MeV
- Analogue or variance reduction calculations

A multipurpose code

The program can be used in different fields such as shielding, dosimetry, high energy experimental physics and engineering, cosmic ray studies, medical physics, etc.

- Each radiation component is treated as far as possible with the same level of accuracy (it's like having 4 different programs in one, for pure neutron, electron-photon or muon problems – and hadrons, of course!)
- FLUKA can be run in fully analog mode, for calorimetry. It can calculate coincidences and anticoincidences
- It can also be run in biased mode, for shielding design

  But also experimental high energy physicists need sometimes to make studies of deep penetration or rare events: hadron punchthrough, radiation background in underground experiments, muon production over short decay lengths

FLUKA History

Beginning of the FLUKA *history : 1962* Johannes Ranft (Leipzig) and H. Geibel (CERN): MonteCarlo codes for high energy beams, as required for CERN accelerators *first phase of SPS design*

The name FLUKA *: 1970*: calorimeter fluctuations on an event-by-event basis (FLUKA = FLUktuierende KASkade).

At the beginning of the 70's, strong contribution of J. Ranft and J. Routti (Helsinki), to the SPS radiation study group, coordinated by K. Goebel. Later, researchers from Helsinki (P. Aarnio) and from CERN (G.R. Stevenson, A. Fassò) contributed to the code till $\approx$ 1987.

The present code : since 1990 mostly INFN-Milan : little or no remnants of older versions. Link with the past: J. Ranft, A. Fassò

The code is huge: $\approx 350,000$ lines of fortran code (vs $\approx 30,000$ in 1987)

FLUKA: sponsors

FLUKA is a "private" effort, it has no official distribution, and is in continuos evolution. Developments are always driven by the concrete needs of the authors experiments/collaborations.

There is no "official" CERN support for FLUKA, even though presently A. Ferrari , A. Fassò and P.R. Sala are working at CERN.

A project for FLUKA development is being discussed by the INFN scientific committees and it is expected to be approved in September.

Supported by a NASA contract for space-related developments.

Wide use at CERN (SL, TIS, CNGS, LHC experiments..) and in other labs (SLAC, INFN..)

MonteCarlo of the ICARUS experiment, part of the Energy Amplifier simulation chain...

The FLUKA hadronic models

Hadron-Nucleon

Elastic, exchange	P<3-5GeV/c	low E π,K	High Energy
Phase shifts,	Resonance prod.	Special	DPM
data,eikonal	and decay		hadronization

Hadron-Nucleus

P<4-5GeV/c	High Energy
PEANUT:	Glauber-Gribov
Sophisticated GINC	multiple interactions
preequilibrium	Coarser GINC

Evaporation/Fission/Fermi break-up

γ deexcitation

Hadron-nucleon interaction models

Elastic, charge exchange and strangeness exchange reactions:

- Available phase-shift analysis and/or fits of experimental differential data
- At high energies, standard eikonal approximations are used

Particle production interactions: two kind of models

- Those based on "resonance" production and decays, which cover the energy range up to 3–5 GeV
- Those based on quark/parton string models, which provide reliable results up to several tens of TeV

Nucleon–nucleon cross sections I

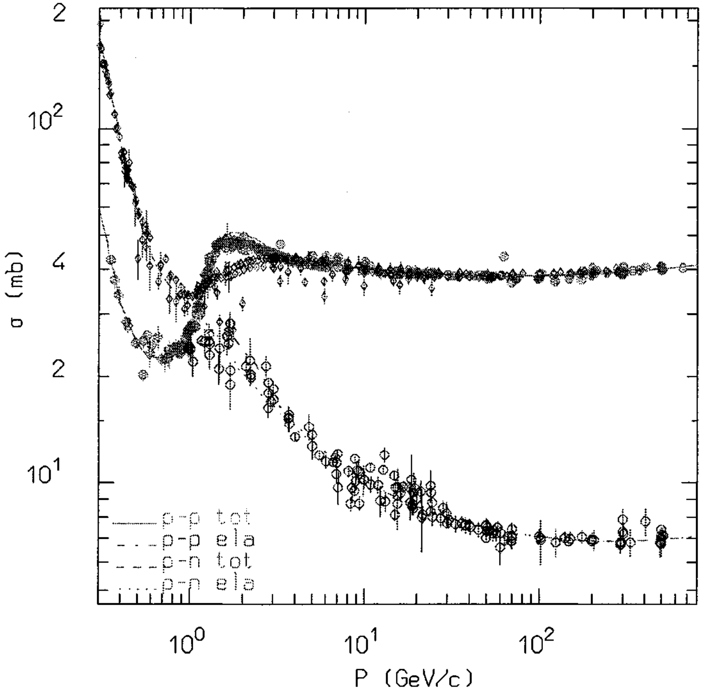

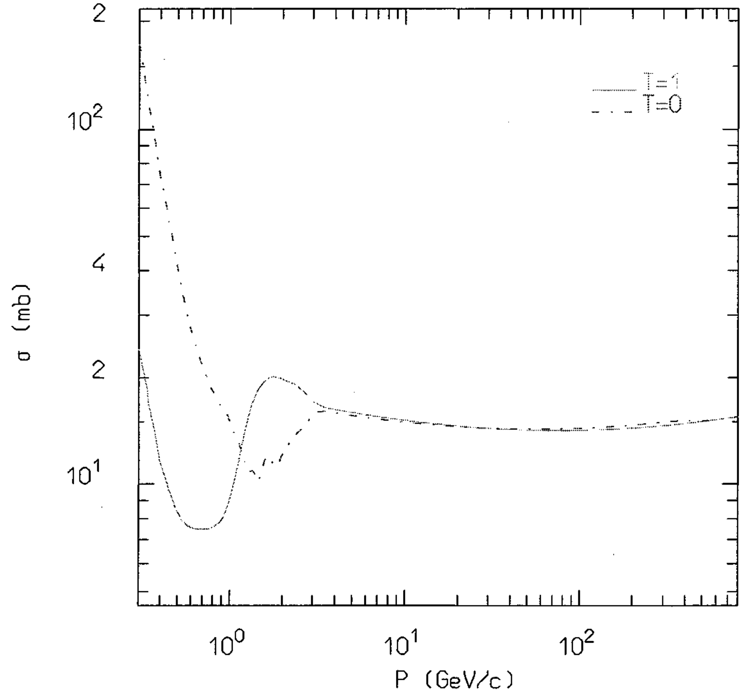

Total and elastic cross section for p–p and p–n scattering, together with experimental data (left), isospin decomposition in the T=0 and T=1 components (right)

Nonelastic hN interactions at intermediate energies

- $N_1 + N_2 \to N_1' + N_2' + \pi$ threshold around 290 MeV, important above 700 MeV,
- $\pi + N \to \pi' + \pi'' + N'$ opens at 170 MeV.

Dominance of the Δ resonance and of the N^* resonances $\to$ reactions treated in the framework of the isobar model $\to$ all reactions proceed through an intermediate state containing at least one resonance.

$$
\begin{aligned}
N_1 + N_2 &\to N_1' + \Delta(1232) \to N_1' + N_2' + \pi \\
\pi + N &\to \Delta(1600) \to \pi' + \Delta(1232) \to \pi' + \pi'' + N' \\
N_1 + N_2 &\to \Delta_1(1232) + \Delta_2(1232) \to N_1' + \pi_1 + N_2' + \pi_2
\end{aligned}
$$

Resonance energies, widths, cross sections, branching ratios from data and conservation laws, whenever possible. Inferred from inclusive cross sections when needed

inelastic hN at high energies: DPM

- Problem: "soft" interactions → no perturbation theory.
- Solution : Interacting strings (quarks held together by the gluon-gluon interaction into the form of a string)
- Interactions treated in the Reggeon-Pomeron framework
- At sufficiently high energies the leading term corresponds to a Pomeron ($I\!P$) exchange (a closed string exchange)
- each colliding hadron splits into two colored partons → combination into two color neutral chains → two back-to-back jets
- Physical particle exchange produce single chains at low energies
- higher order contributions with multi-Pomeron exchanges important at $E_{lab} \geq$ 1 TeV

DPM: chain examples

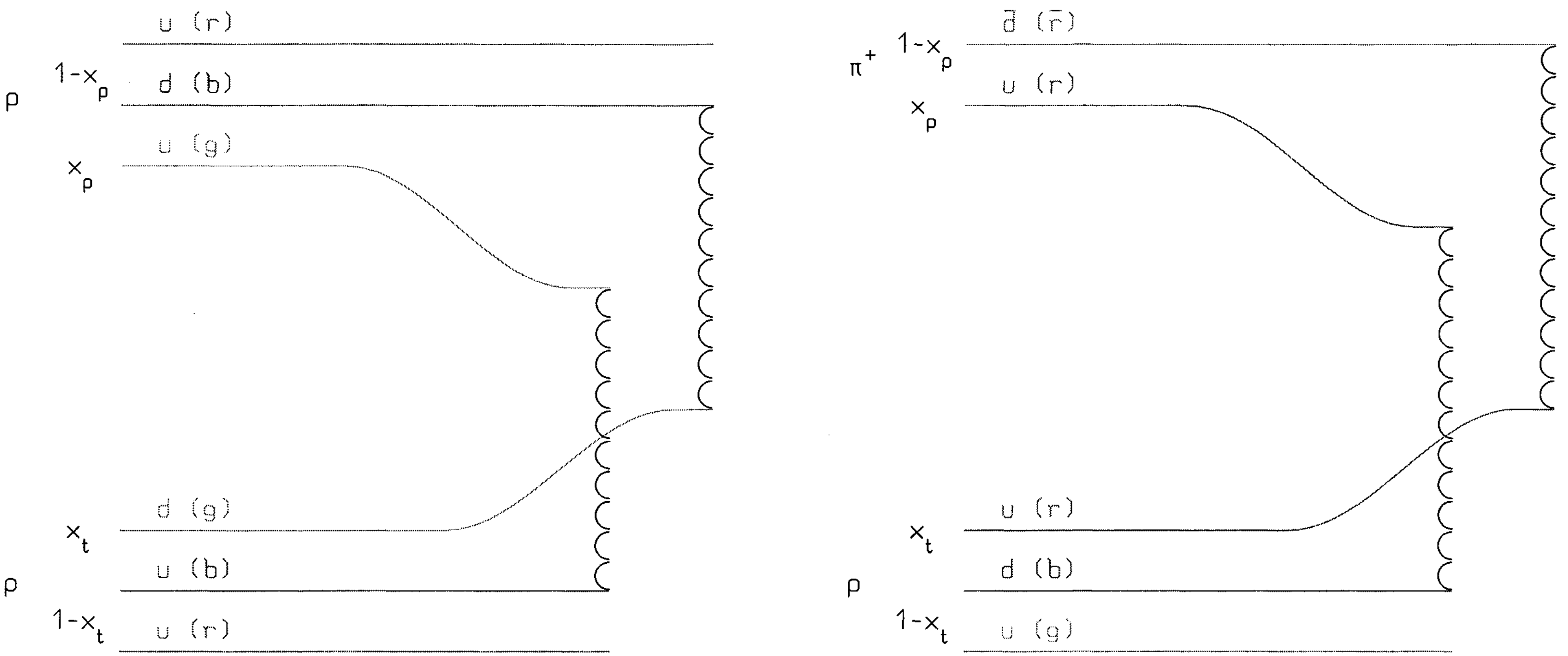

Leading two-chain diagrams in DPM for $p - p$ (left) and $\pi - p$ (right) scattering. The color (red, blue, and green) and quark combinations shown in the figure are just one of the allowed possibilities

DPM and fragmentation

from DPM:

- Number of chains
- Chain composition
- Chain energies and momenta
- Diffractive events

Almost No Freedom

Chain hadronization

- Assumes chain universality
- Fragmentation functions from hard processes and e^+e^-
- Transverse momentum from e^{-bm_T} behaviour
- Mass effects at low energies

The same functions and (few) parameters for all reactions and energies

hA at high energies: GLAUBER Cascade

Elastic, Quasi-elastic and Absorption hA cross sections derived from Free hadron-Nucleon cross section + Nuclear ground state ONLY .
Inelastic interaction $\equiv$ multiple interaction with ν target nucleons, with binomial distribution:

$$P_{r\ \nu}(b) \equiv \binom{A}{\nu} P_r^{\nu}(b)\left[1 - P_r(b)\right]^{A-\nu}$$

where $P_r(b) \equiv \sigma_{hN\ r} T_r(b)$, and $T_r(b)$=folding of nuclear density and scattering profiles along the path.
On average :

$$< \nu >= \frac{Z\sigma_{hp\ r} + N\sigma_{hn\ r}}{\sigma_{hA\ abs}}$$

$$\sigma_{hA\ abs}(s) = \int \mathrm{d}^2\vec{b}\left[1 - \left(1 - \sigma_{hN\ r}(s) T_r(b)\right)^A\right]$$

h-A at high energies: Glauber-Gribov

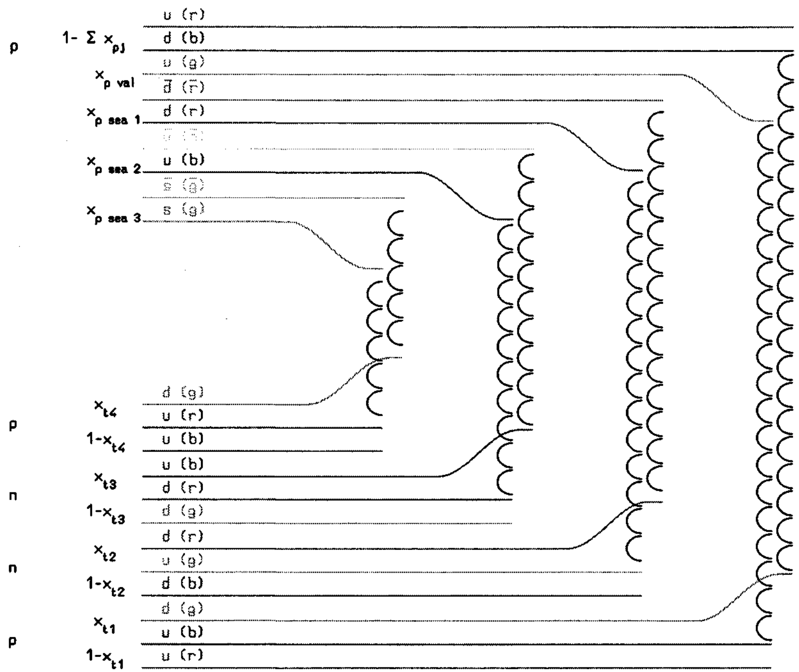

One of the possibilities for Glauber-Gribov scattering with 4 collisions

Gribov

$\Downarrow$

2ν chains

2 valence-valence chains

$2(\nu - 1)$ chains between projectile sea and target valence (di)quarks.

No freedom, except in mass effects at low energies.

Fermi motion included $\rightarrow$ smearing of E and p_T distributions

Recent improvements in the high energy model

G. Collazuol, A. Ferrari, A. Guglielmi and P.R. Sala, NIM A 449 (2000), 609

The DPM + Glauber model embedded into old FLUKAversions (and in *GEANT-FLUKA*) had important limitations:

- Glauber cascade described at an elementary level;
- all resonances assumed on mass shell;
- coarse chain hadronization, and no particular attention to threshold and finite mass effects;
- isospin conservation not enforced at each individual hadron production step;
- transverse motion reasonable but still far from satisfactory;
- simplified description of diffractive processes.

Recent improvements in the high energy model

All improved along the years. Most critical point: chain hadronization

- Threshold and finite mass effects checked against low energy data (chains with 2 or 3 had.)
- Fragmentation functions checked against 16-450 GeV h-N and h-A data
- Constraint: hadron multiplicity at 200 GeV.
- Balanced optimization: better SPY agreement could be achieved, spoiling low energy data.

Comparison with SPY I

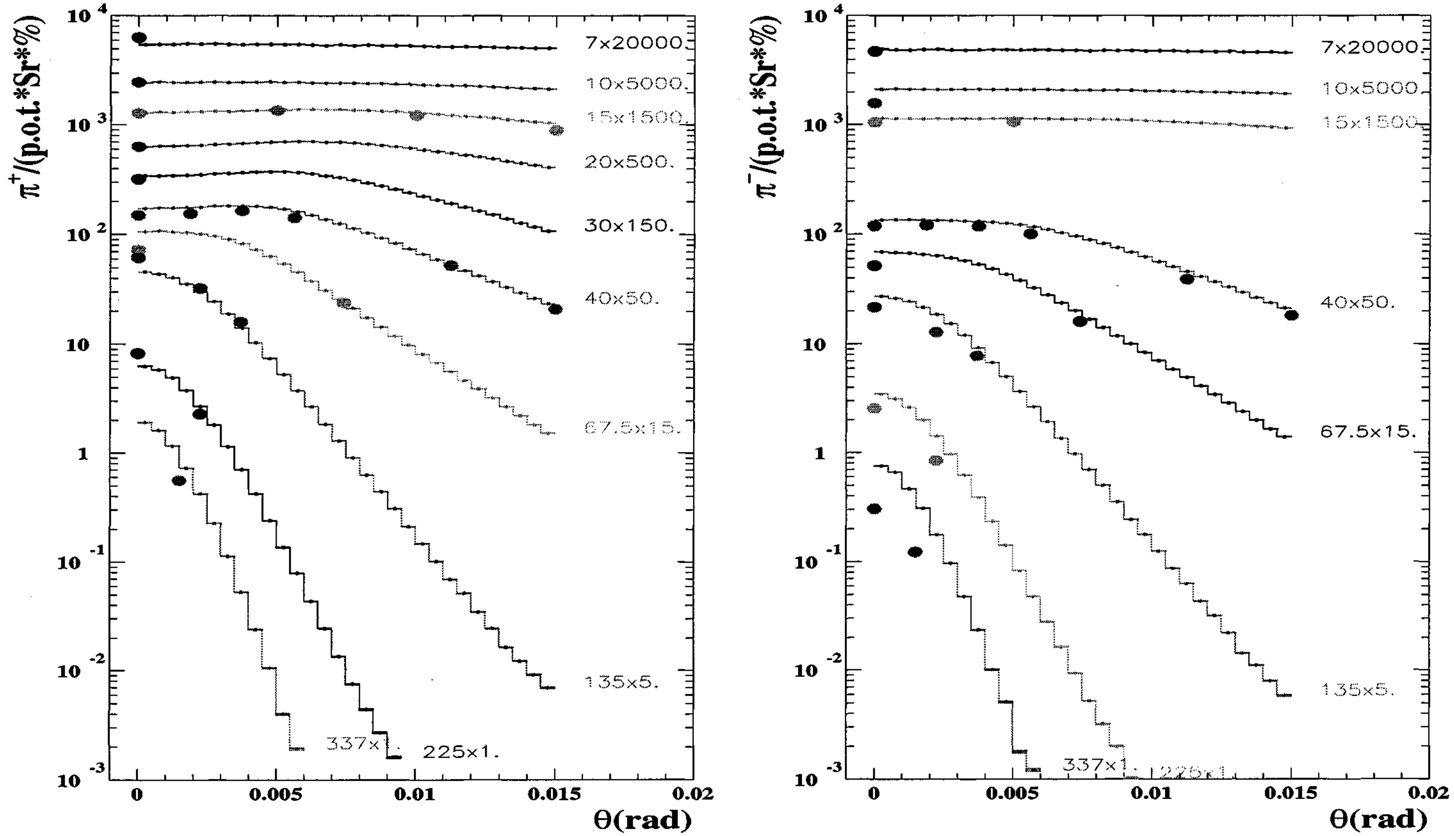

Double differential cross section for π^+ (left) and π^- (right) production for 450 GeV/c protons on a 10 cm thick Be target (data from H.W. Atherton CERN 80–07, G. Ambrosini et al. PL B425 208 (1988)).

Nonelastic hA interactions at high energies: examples

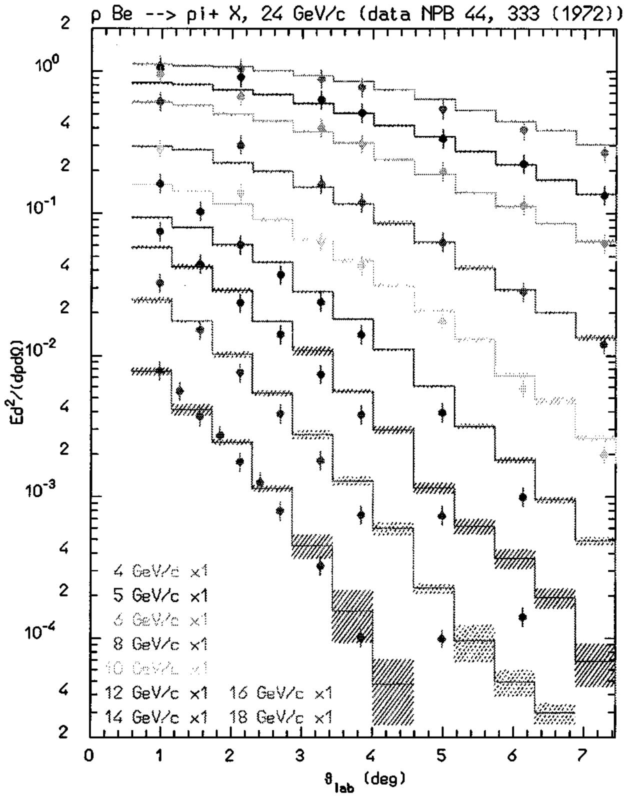

Invariant cross section distribution for π^+, 24 GeV/c protons on Be (T.Eichten et al. NPB 44, 333 (1972)).

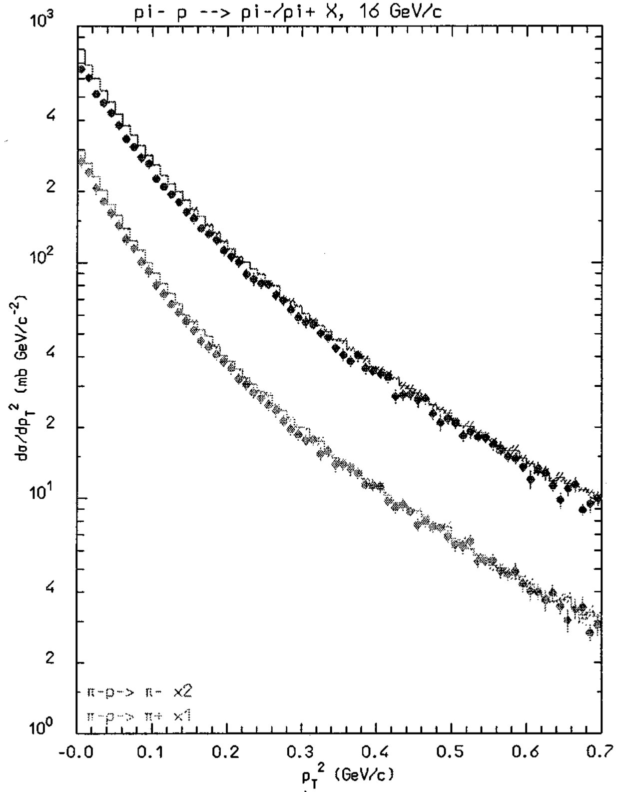

p_T spectra of π^+ and π^- produced by 16 GeV/c π^- on H. (M.E Law et al. LBL80 (1972)).

Nonelastic hA interactions at high energies: examples

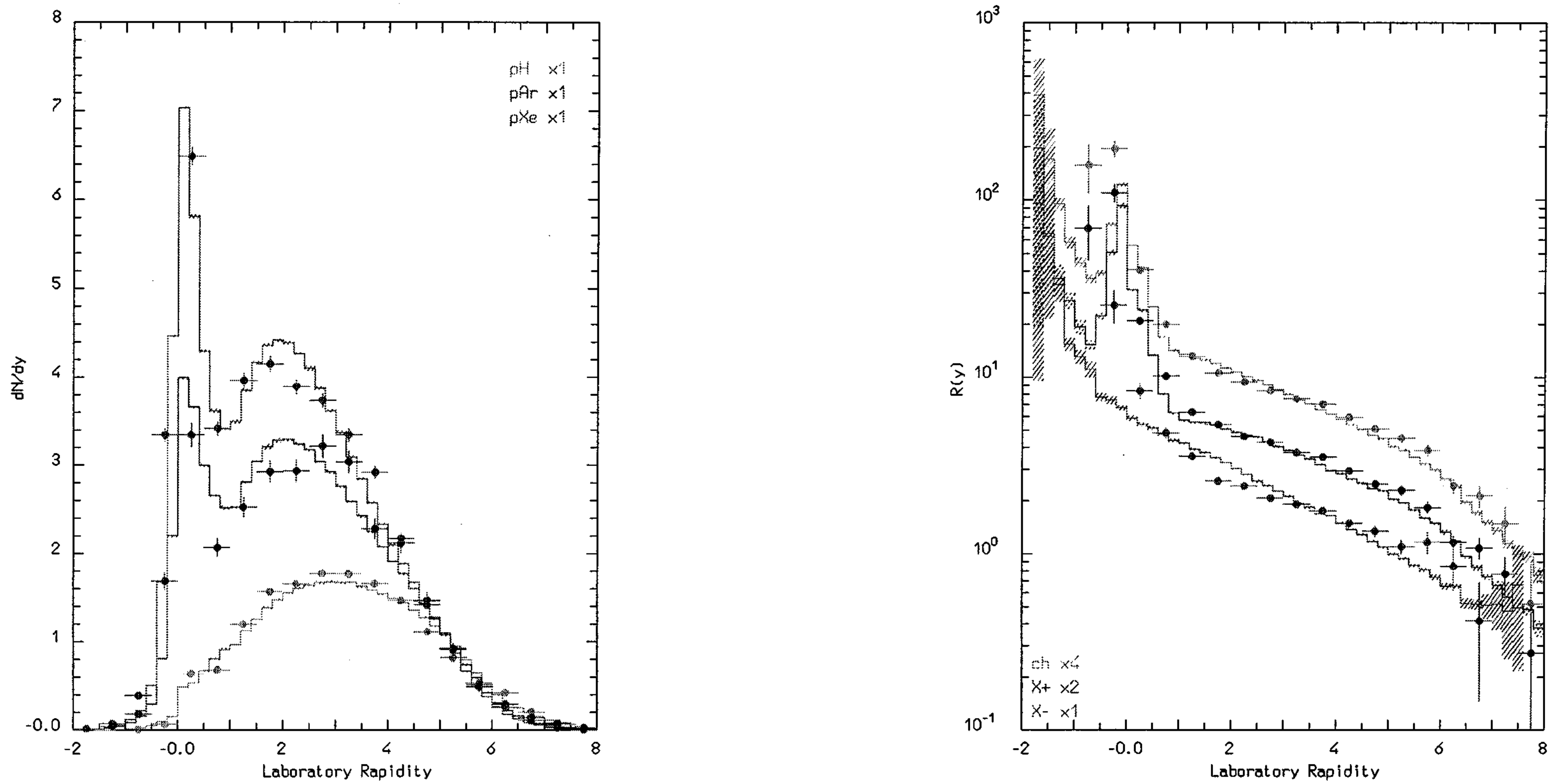

Rapidity distribution of charged particles produced in 200 GeV proton collisions on Hydrogen, Argon, and Xenon target (left) and ratio of rapidity distribution of charged, positive, and negative particles produced in 200 GeV proton collisions on Xenon and Hydrogen (right). Data from C. De Marzo et al., PRD26, 1019 (1982).

CERN Neutrino to GranSasso

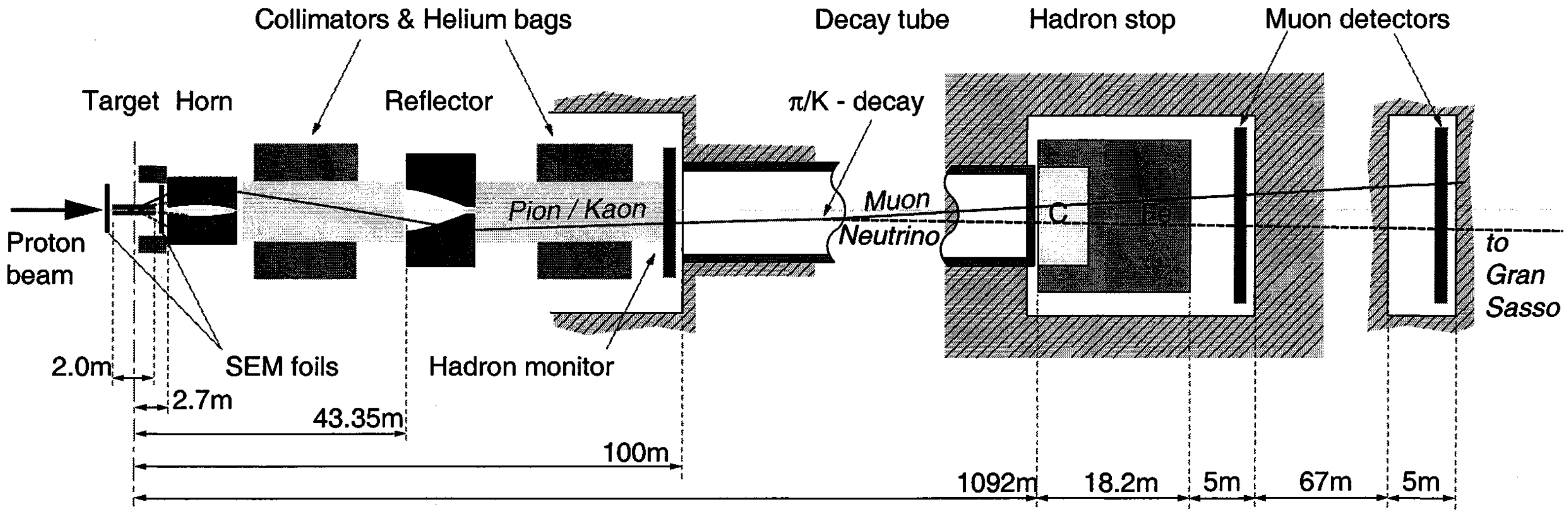

400 GeV/c protons, double fast extraction, $5\ 10^{13}$ protons every 6 s

Thin graphite target (⊘4 mm, 13 bars 100 mm each)

Two magnetic lenses focalize 35 and 50 GeV positive

1 Km decay tube

730 Km to Gran Sasso

Nice agreement with experiment → confidence in prediction for CNGS

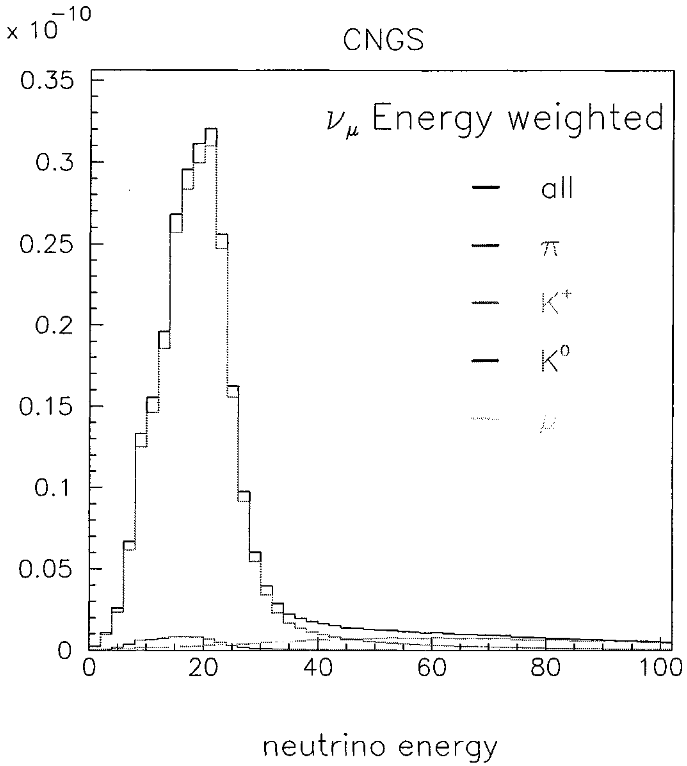

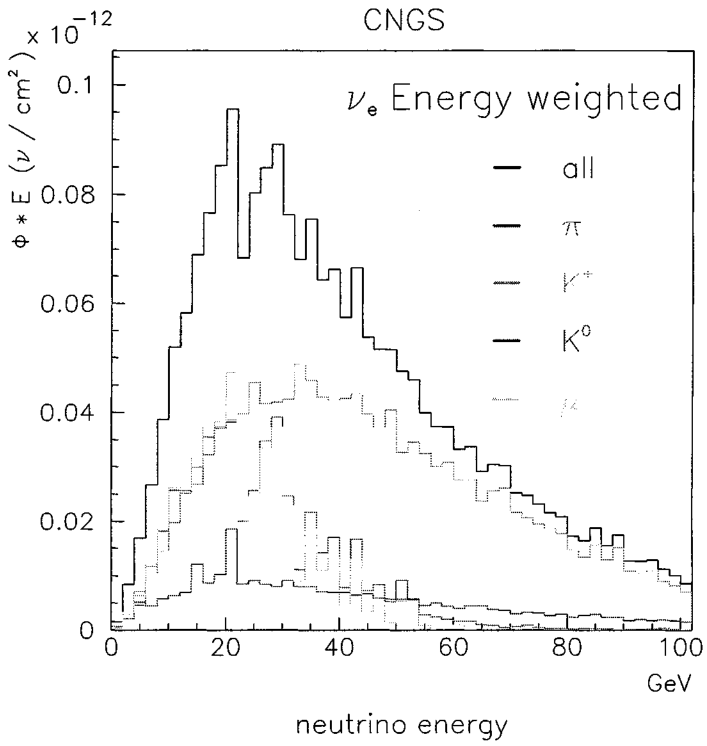

Neutrino quasi-elestic events

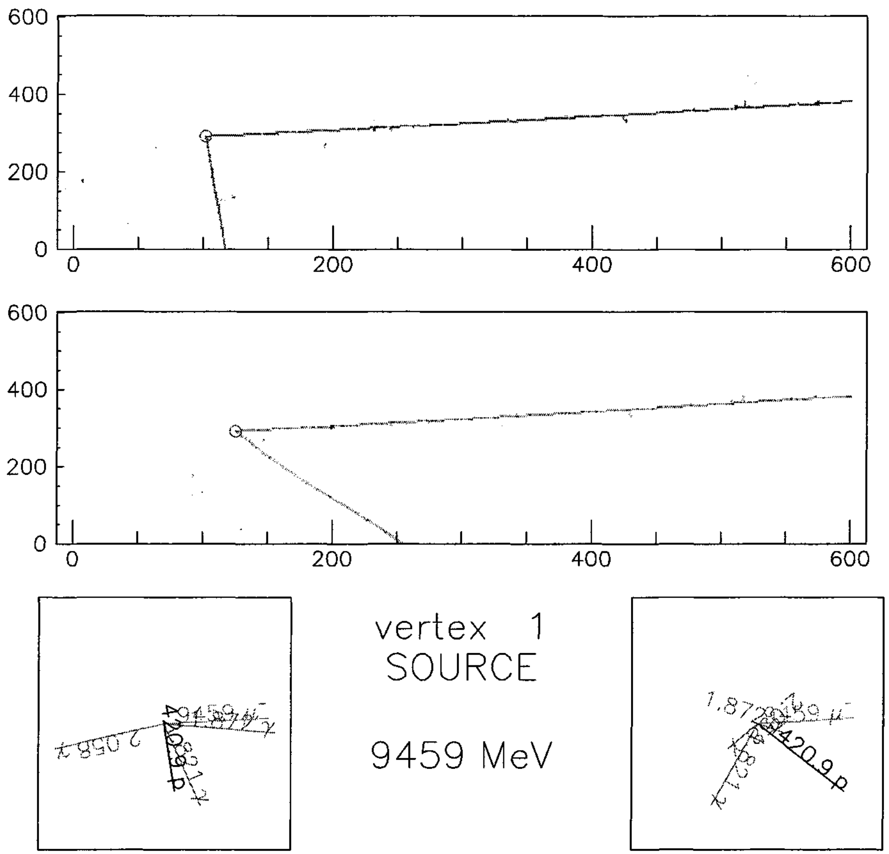

ICARUS prototype: two views in Liqid Argon, 10 GeV ν_μ CC

"Clean" event :

$$\nu_\mu\, n \rightarrow \mu^- \; p$$
$$\downarrow$$
$$\mu^- \; \mathrm{p}\; \gamma$$

Neutrino quasi-elestic events

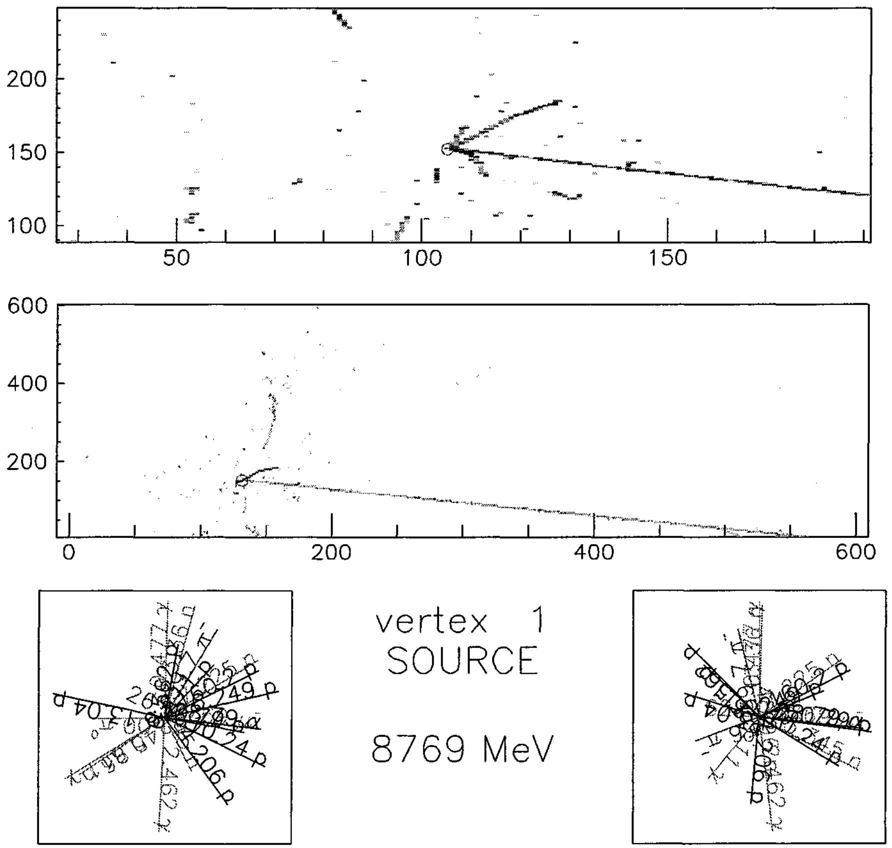

ICARUS prototype: two views in Liqid Argon, 10 GeV ν_μ CC

Complex event :

$$\nu_\mu\, n \rightarrow \mu^-\, p$$

$$\downarrow$$

1 μ^-, 8 p, 2 π^-, 1 π^0, 4 n, 1 α, 3 γ

(Generalized) IntraNuclear Cascade basic assumptions

1. Primary and secondary particles moving in the nuclear medium
2. *Target nucleons motion and nuclear well according to the Fermi gas model*
3. Interaction probability from σ_{free} + Fermi motion $\times$ $\rho(r)$ + exceptions (ex. π)
4. *Glauber cascade at high energies*
5. Classical trajectories (+) nuclear mean potential (*resonant for* π*'s!!*)
6. Curvature from nuclear potential $\rightarrow$ refraction and reflection.
7. Interactions are incoherent and uncorrelated
8. Interactions in projectile–target nucleon CMS $\rightarrow$ Lorentz boosts
9. *Multibody absorption for* π, μ^-, K^-
10. *Quantum effects (Pauli, formation zone, correlations...)*
11. *Exact conservation of energy, momenta and all additive quantum numbers,including nuclear recoil*

Formation Zone

Naively: "materialization" time. Qualitative estimate: in the frame where $p_{\|} = 0$

$$\bar{t} = \Delta t \approx \frac{\hbar}{E_T} = \frac{\hbar}{\sqrt{p_T^2 + M^2}}$$

particle proper time

$$\tau = \frac{M}{E_T}\bar{t} = \frac{\hbar M}{p_T^2 + M^2}$$

Going to lab system

$$t_{lab} = \frac{E_{lab}}{E_T}\bar{t} = \frac{E_{lab}}{M}\tau = \frac{\hbar E_{lab}}{p_T^2 + M^2}$$

As a function of particle rapidity y

$$t_{lab} = \bar{t}\cosh y = \frac{\hbar}{\sqrt{p_T^2 + M^2}}\cosh y$$

Condition for possible reinteraction inside a nucleus:

$$v \cdot t_{lab} \leq R_A \approx r_0 A^{\frac{1}{3}}$$

"Coherence length"

Coherence length $\equiv$ formation time for elastic or quasielastic interactions.

Given a two body interaction between with four-momentum transfer

$$q = p_{1i} - p_{1f}$$

the energy transfer seen in a frame where the particle 2 is at rest is given by

$$\Delta E_2 = \nu_2 = \frac{q \cdot p_{2i}}{m_2}$$

From the uncertainty principle this ΔE corresponds to a indetermination in proper time given by $\Delta\tau \cdot \Delta E_2 = \hbar$, that boosted to the lab frames gives a coherence length

$$\Delta x_{lab} = \frac{p_{2lab}}{m_2} \cdot \Delta\tau = \frac{p_{2lab}}{m_2}\frac{\hbar}{\nu_2}$$

And analogue for particle 1

Can be applied also to $\nu - h$ interactions

Nucleon Fermi Motion

Fermi gas model: Nucleons = Non-interacting Constrained Fermions

$$\text{Momentum distribution} \propto \frac{\mathrm{d}N}{dk} = \frac{|k|^2}{2\pi^2}$$

for k up to a (local) Fermi momentum $k_F(r)$ given by

$$k_F(r) = \left[3\pi^2 \rho_N(r)\right]^{\frac{1}{3}}, \quad \rho_N = \textit{neutron or proton density}$$

The Fermi energy ($k_F \approx 1.36\ fm$, $E_F \approx 260\ MeV$ at nuclear max. density) is customarily used in building a sefl-consistent Nuclear Potential

$$\Downarrow$$

Depth of the potential well $\equiv$ Fermi Energy + Nucleon binding Energy

Effect on hadron-nucleon interactions

Smearing of momentum distributions

Smearing of the center of mass energy

Origin of the residual nuclear excitation

Positive Kaons: A probe of Fermi distribution

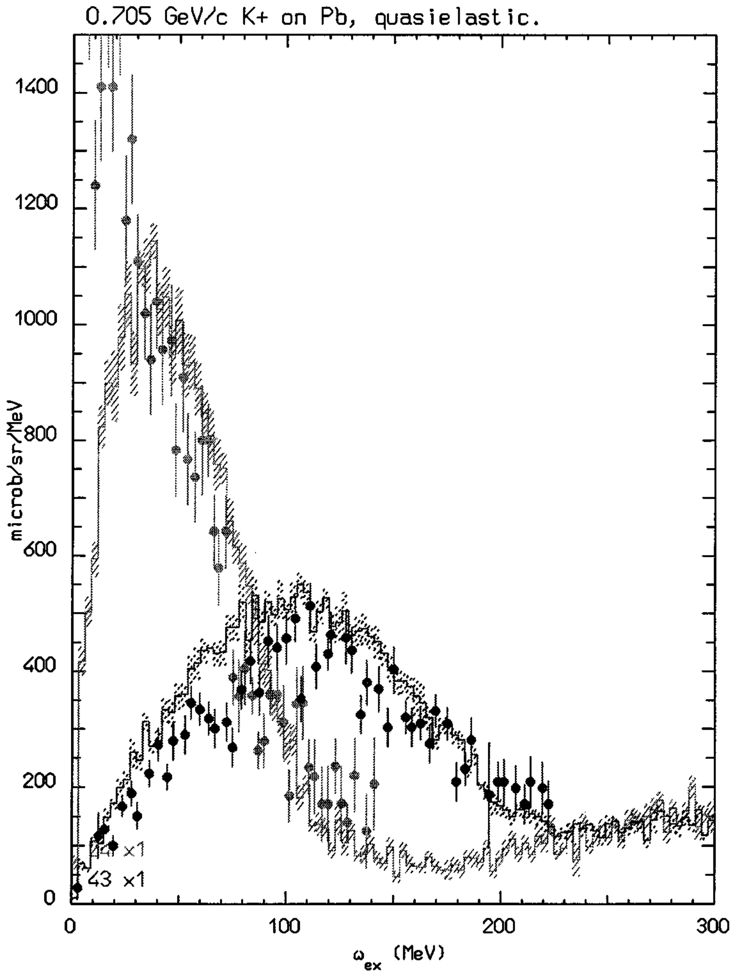

K^+ K^0

No low mass S=1 baryons $\rightarrow$ weak K^+N interaction only elastic and ch. exch. up to ≈ 800 MeV/c

$(K^+, K^{+\prime})$ on Pb vs residual excitation, 705 MeV/c, at $24°$ and $43°$. Histo: FLUKA, dots: data (Phys. Rev. C51, 669 (1995))

On free nucleon: recoil energy :
43 MeV at $24°$, 117 MeV at $43°$.

π–nucleon cross sections

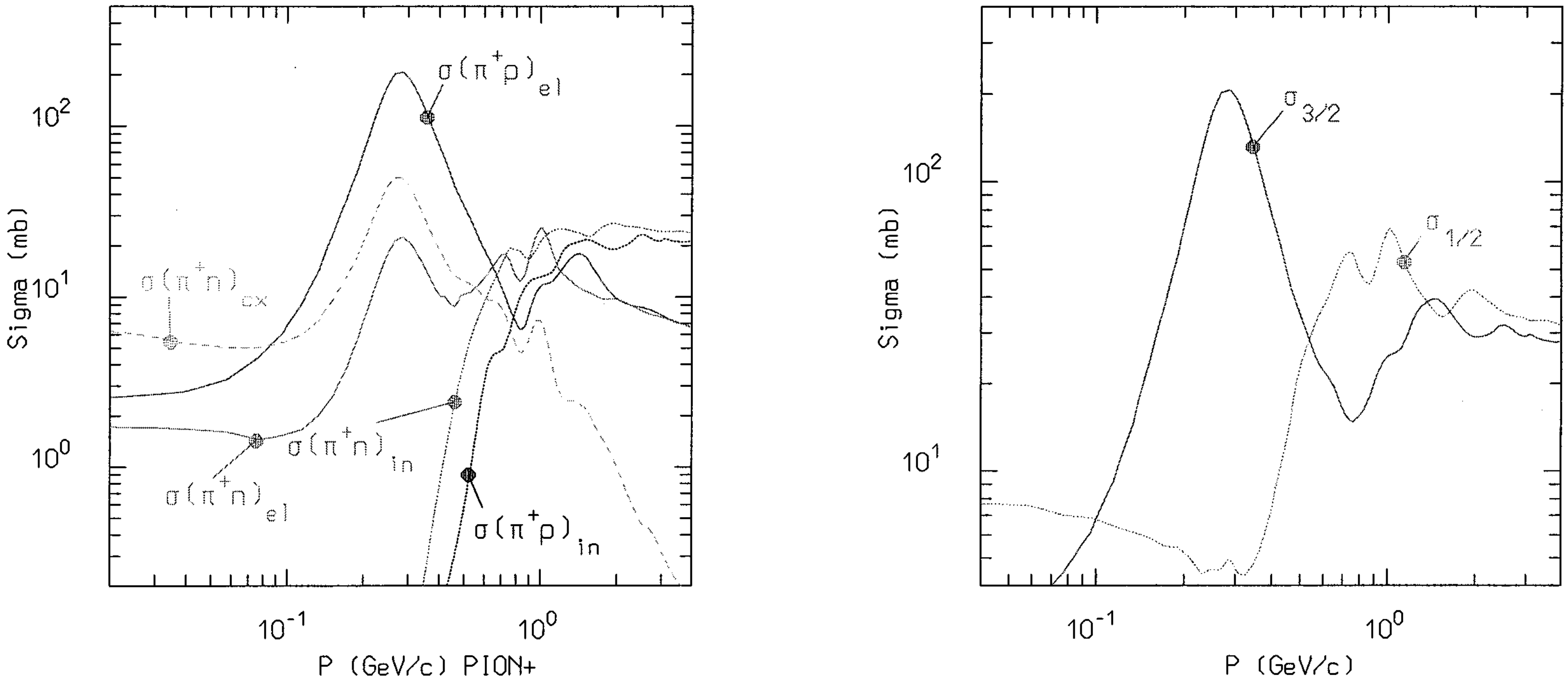

Elastic, chx and inel. cross sections for π–N scattering (left), isospin decomposition in the T=1/2 and T=3/2 components (right)

Pions: nuclear medium effects

Pion-nucleon interactions: non-resonant channel and p-wave resonant formation of Δ's. In nuclear medium Δ's can either decay, resulting in elastic scattering or charge exchange, or interact with other nucleons, resulting in pion absorption $\rightarrow$ the width of the resonance is thus different from the free one and the free pion-nucleon cross section must be modified according to

Assuming a Breit-Wigner for the free resonant cross section with width Γ_F

$$\sigma_{res}^{Free} = \frac{8\pi}{p_{cm}^2} \frac{M_\Delta^2 \Gamma_F(p_{cm})^2}{\left(s - M_\Delta^2\right)^2 + M_\Delta^2 \Gamma_F(p_{cm})^2}$$

An "in medium" resonant cross section σ_{res}^A can be obtained adding to Γ_F the imaginary part of the (extra) width arising from nuclear medium effects:

$$\frac{1}{2}\Gamma_T = \frac{1}{2}\Gamma_F - \mathrm{Im}\Sigma_\Delta, \quad \Sigma_\Delta = \Sigma_{qe} + \Sigma_2 + \Sigma_3$$

(Σ_{qe}, Σ_2, Σ_3 = widths for quasielastic scattering, two and three body absorption)
The effective in-nucleus cross section is then obtained taking also into account a further two-body s-wave absorption cross section derived from the optical model

$$\sigma_t^A = \sigma_{res}^A + \sigma_t^{Free} - \sigma_{res}^{Free} + \sigma_s^A, \quad \sigma_s^A(\omega) = \frac{4\pi}{p}\left(1 + \frac{\omega}{2m}\right)\mathrm{Im}B_0(\omega)\rho$$

Microscopic pion absorption cross sections

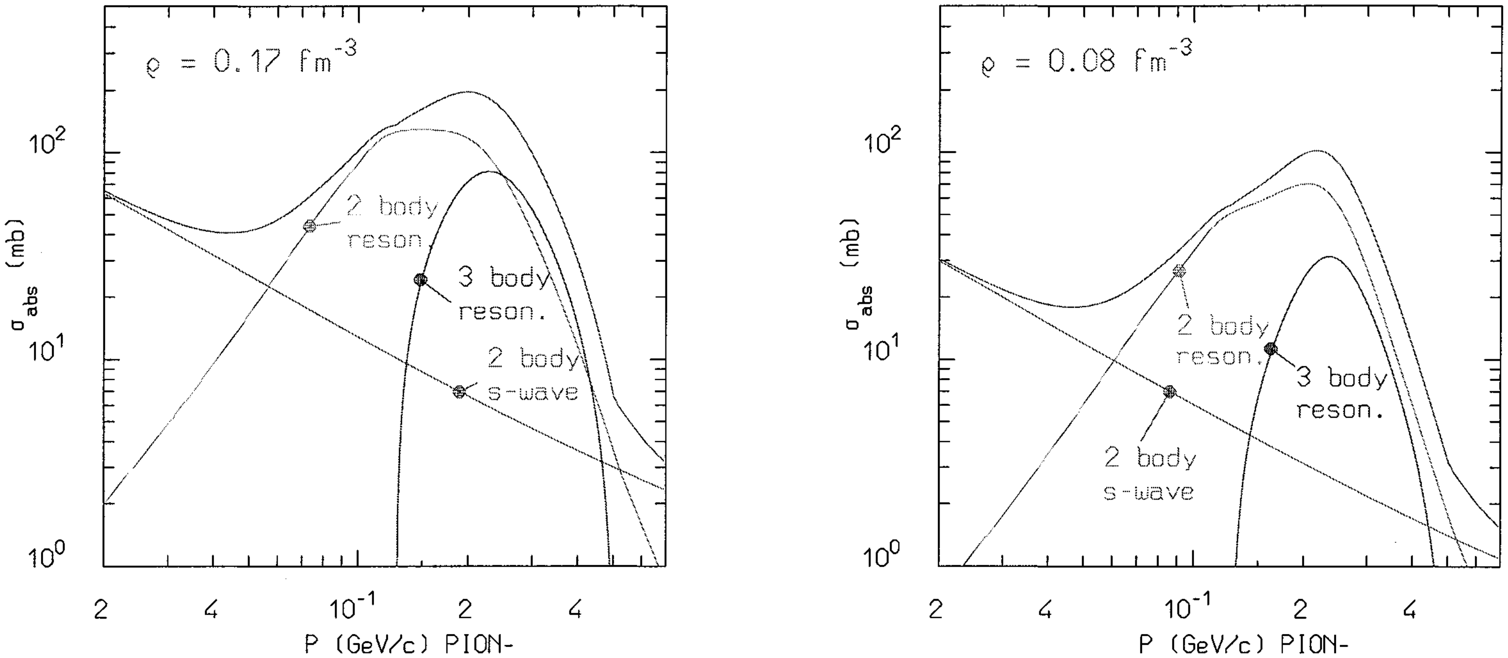

Charged pion absorption cross section for infinite symmetric nuclear matter at two different density values ($\lambda_{abs}^{-1} = \sigma_{abs} \cdot \frac{1}{2}\rho = \sigma_{abs} \cdot \rho_{pro} = \sigma_{abs} \cdot \rho_{neu}$)

Pions: optical potential

For pions, a complex nuclear potential can be defined out of the pion-nucleon scattering amplitude to be used in conjunction with the Klien-Gordon equation:

$$\left[(\omega - V_c)^2 - 2\omega U_{opt} - K^2\right]\Psi \;=\; m_\pi^2\Psi$$

In coordinate space, this is written as (the upper/lower signs refer to π^+/π^-):

$$2\omega U_{opt}(\omega, r) \;=\; -\beta(\omega, r) + \frac{\omega}{2M}\nabla^2\alpha(\omega, r) - \nabla\cdot\frac{\alpha}{1+g\alpha(\omega, r)}\nabla$$

$$\beta \;=\; 4\pi\left[\left(1+\frac{\omega}{M}\right)\left(b_0(\omega) \mp b_1(\omega)\frac{N-Z}{A}\right)\rho(r) + \left(1+\frac{\omega}{2M}\right)B_0(\omega)\rho^2(r)\right]$$

$$\alpha \;=\; 4\pi\left[\frac{1}{1+\frac{\omega}{M}}\left(c_0(\omega) \mp c_1(\omega)\frac{N-Z}{A}\right)\rho(r) + \frac{1}{1+\frac{\omega}{2M}}C_0(\omega)\rho^2(r)\right]$$

Using standard methods to get rid of the non-locality, in momentum space

$$2\omega U_{opt}(\omega, K) \;=\; -\beta - K^2\frac{\alpha}{1+g\alpha} + \frac{\omega}{2M}\nabla^2\alpha$$

$$K^2 \;=\; k_0^2 + V_c^2 - 2\omega V_c^2 - 2\omega U_{opt}(\omega, K) = \frac{k_0^2 + V_c^2 - 2\omega V_c^2 + \beta - \frac{\omega}{2M}\nabla^2\alpha}{1-\bar{\alpha}}$$

$$\bar{\alpha} \;=\; \frac{\alpha}{1+g\alpha}$$

Pion optical potential examples

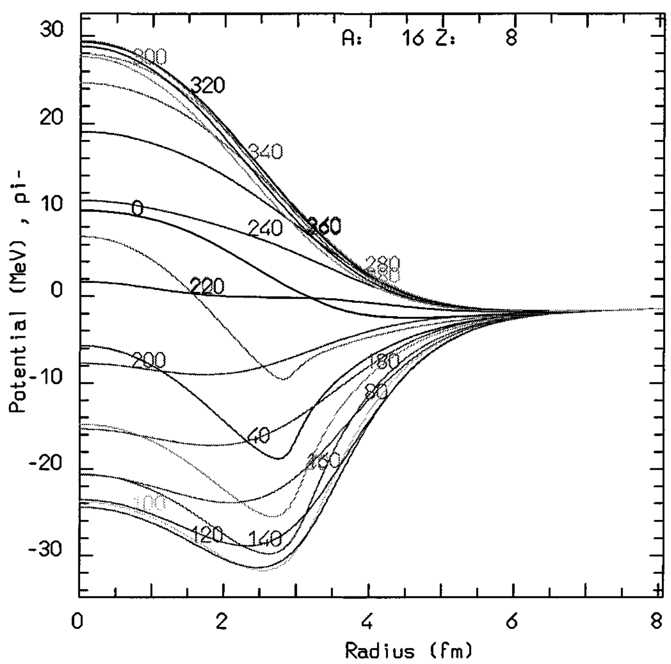

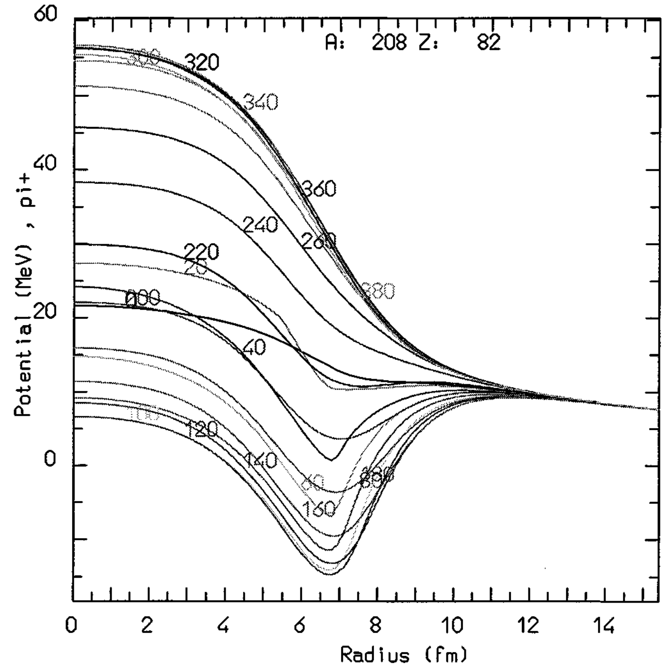

The real part of the pion optical potential for π^- on ^{16}O (left) and π^+ on ^{208}Pb (right) as a function of radius for various pion energies (MeV)

Pion absorption cross sections: examples

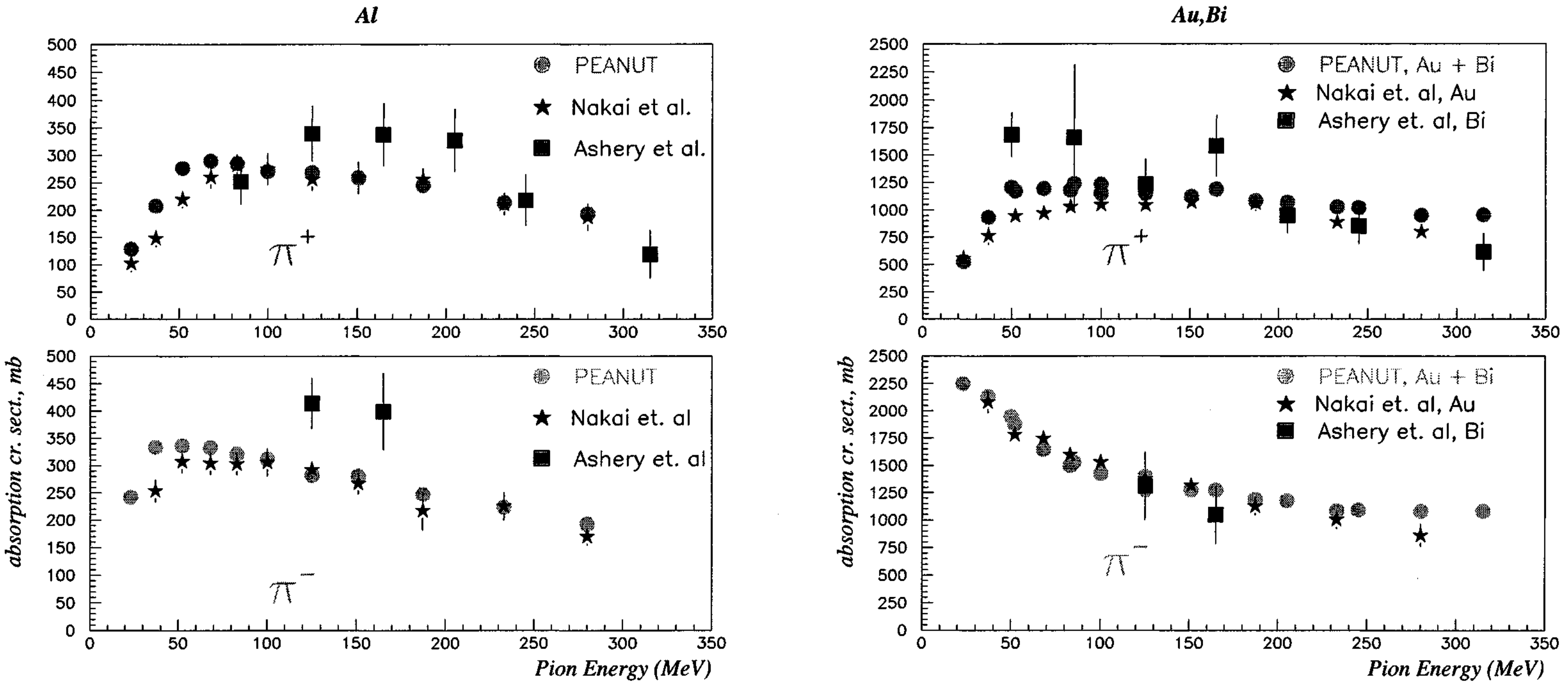

Computed and exp. pion absorption cross section on Aluminum as a function of energy

Computed and exp. pion absorption cross section on Gold or Bismuth as a function of energy

(Exp. data: D. Ashery et al., **PRC23**, (1981) 2173 and K. Nakai et. al., **PRL44**, (1979) 1446)

Pion-nucleus interactions: examples

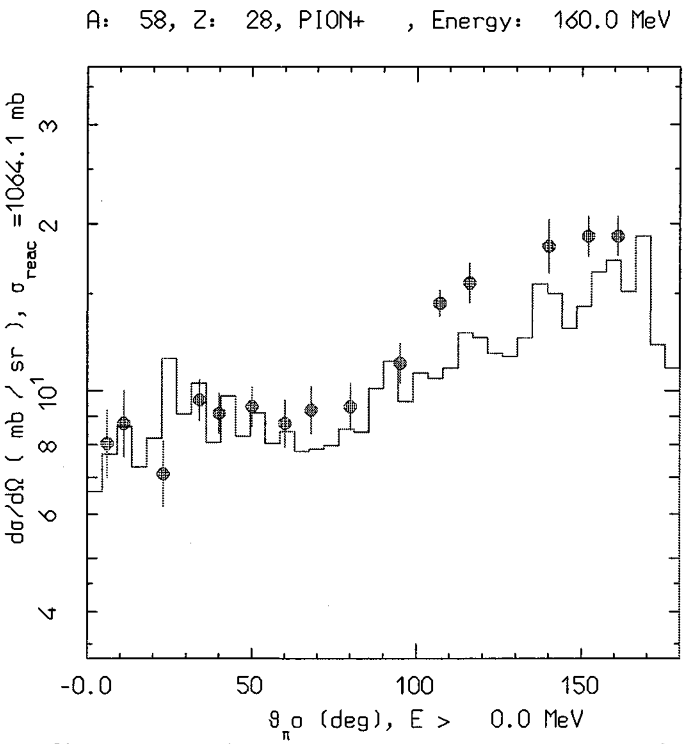

Computed and exp. pion charge exchange angular distribution for $^{58}Ni(\pi^+,\pi^0)$ at 160 MeV

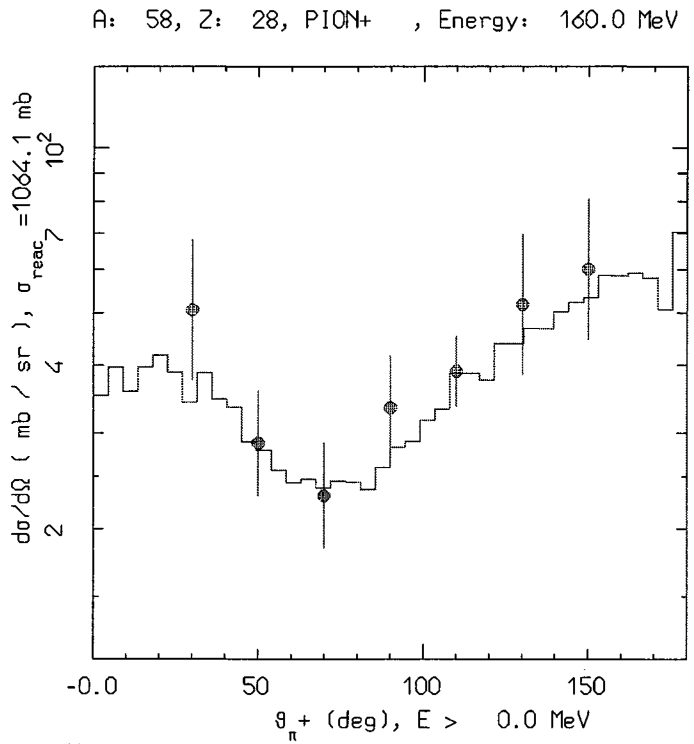

Computed and exp. pion inelastic angular distribution for $^{58}Ni(\pi^+,\pi^{+'})$ at 160 MeV

(Exp. data: W.J. Burger et al., **PRC41**, *(1990) 2215 and R.D. McKeown et al.,***PRC24**, *(1981) 211)*

K^- $\bar{K}^0$ -nucleon interactions at medium-low energies

Plenty of S=1 baryonic resonances at low energies

$\Lambda\pi$ and $\Sigma\pi$ channels already open at rest

$\rightarrow$ Strong K^-N interaction

Multichannel analisys needed

Many partial waves contribute

Kaon nuclear potential non-negligible

Hyperons can be bound in nuclei

In PEANUT: in progress

Multichannel partial wave expansion

s wave at low momenta [1];

$0 < l < 5$ up to 1.8 GeV/c [2]

Isospin relations to link different charge states

Mass differences taken into account (charge exchange)

[1] A.D. Martin, Nuc.Phys. B179 (1981) 33

[2] G.P. Gopal et al., Nuc. Phys. B119(1977),362

Kaon-nucleon interactions examples

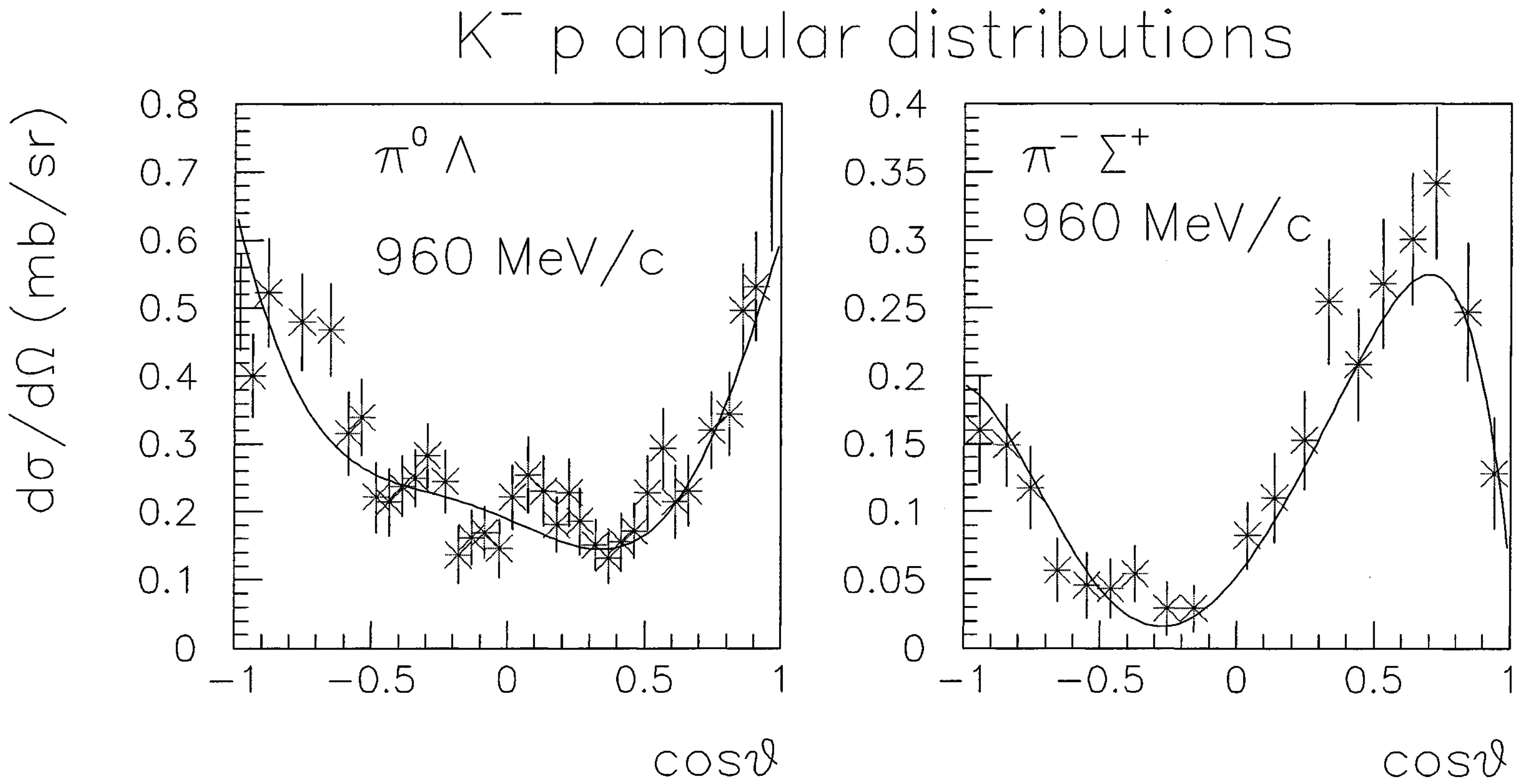

Line: FLUKA, partial wave expansion, symbols: exp. data from B.R. Martin and M.K. Pidkok, Nucl. Phys. B126 (1977) 266

Preequilibrium

For E $>$ π production threshold $\rightarrow$ only (G)INC models

At lower energies$\rightarrow$ a variety of preequilibrium models

Two leading approaches

the quantum-mechanical multistep model	the exciton model
Very good theoretical background	statistical assumptions
complex, difficulties for multiple emission	simple and fast

Exciton model: chain of steps, each (n_{th}) step corresponding to N_n

"excitons" $==$ either a particle above or a hole below the Fermi surface

Statistical assumption: any partition of the excitation energy E among N,

$N = N_h + N_p$, excitons has the same probability to occur

Step: nucleon-nucleon collision with $N_{n+1} = N_n + 2$ ("never come back" approximation)

Chain end = equilibrium = N_n sufficiently high or excitation energy below threshold

N_1 depends on the reaction type and on the cascade history

Preequilibrium : GDH

Preequilibrium emission probability:

$$P_{x,n}(\epsilon)d\epsilon = \sum n_{p_x} \frac{\rho_n(U,\epsilon)gd\epsilon}{\rho_n(E)} \frac{r_c(\epsilon)}{r_c(\epsilon)+r_+(\epsilon)}$$

where the density (MeV^{-1}) of exciton states is given by:

$$\rho_n(E) = \frac{g(gE)^{n-1}}{n!(n-1)!}$$

the emission rate in the continuum:

$$r_c = \sigma_{inv} \frac{\epsilon}{g_x} \frac{(2s+1)\,8\pi m}{h^3}$$

and the reinteraction rate:

$$r_+(\epsilon) \;=\; f_{Pauli}(\epsilon, E_F)\,[\rho_p\sigma_{xp} + \rho_n\sigma_{xn}]\left[\frac{2(\epsilon+V)}{m}\right]^{1/2}$$

$$(or\ from\ optical\ potential)$$

GDH: ρ,E_F are "local" averages on the trajectory and constrained exciton state densities are used for the lowest lying exciton configurations.

Preequilibrium: modified GDH in PEANUT

- σ_{inv} from systematics
- Correlation/formation zone / hardcore effect on reinteractions:

$$\frac{r_c(\epsilon)}{r_c(\epsilon)+r_+(\epsilon)} \rightarrow P_c^{(h\tau)} + P_c^{(co)} + P_c^{(std)}$$

$$\begin{aligned}
P_c^{(h\tau)} &= escape\ prob.\ in\ zone\ = max(\tau, hardcore) \equiv h\tau \\
P_c^{(co)} &= escape/total\ prob.\ in\ zone\ = (correlation\ -\ h\tau) \\
&\quad (here\ reinteraction\ only\ on\ \mathrm{non}-correlated\ nucleon\ specie\ ) \\
P_c^{(std)} &= \text{"}standard\text{"}\ escape/total\ in\ remaining\ zone.
\end{aligned}$$

- Constrained exciton state densities configurations 1p-1h, 2p-1h, 1p-2h, 2p-2h, 3p-1h and 3p-2h
- Energy dependent form for g_x

Preequilibrium: modified GDH in PEANUT II

- Position dependent parameters = point like values :
  - first step : n_h holes generated in the INC step at positions $\vec{x}_i$:

$$\rho^{loc}_{n_h} = \frac{\Sigma_{i=1}^{n_h} \rho(\vec{x}_i)}{n_h} \qquad E^{loc}_{F\,n_h} = \frac{\Sigma_{i=1}^{n_h} E_F(\vec{x}_i)}{n_h}$$

  - When looking at reinteraction: consider neighborhood:

$$\rho^{nei}_{n_h} = \frac{n_h \rho^{loc}_{n_h} + \rho^{ave}}{n_h + 1} \qquad E^{nei}_{F\,n_h} = \frac{n_h E^{loc}_{F\,n_h} + E^{ave}_F}{n_h + 1}$$

  - Subsequent steps: go towards *ave*rage quantities

$$\rho^{loc}_{n_h+1} = \rho^{nei}_{n_h} \qquad E^{loc}_{F\,n_h+1} = E^{nei}_{F\,n_h}$$

Preequilibrium/(G)INC transition

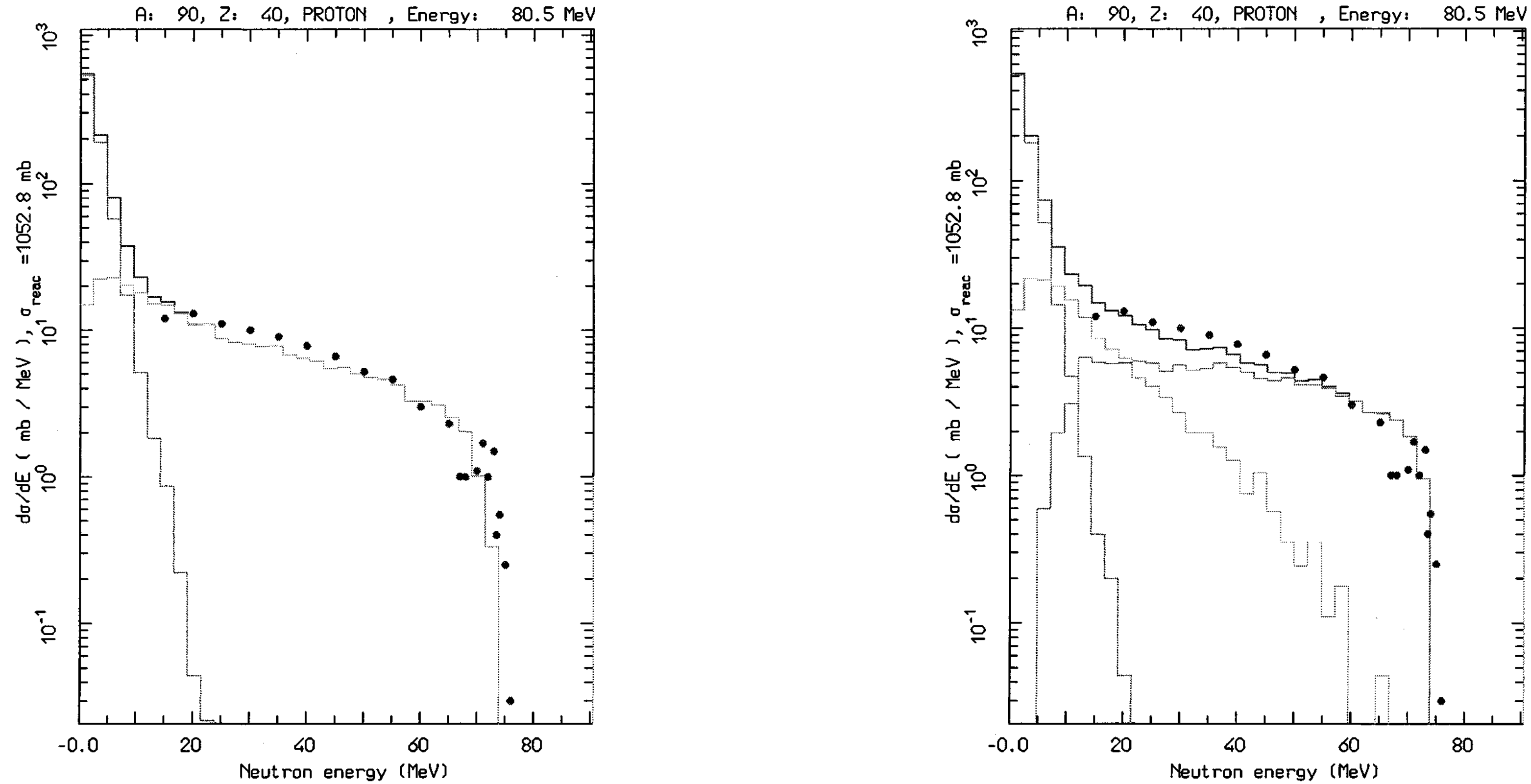

Example of angle integrated ^{90}Zr(p,xn) at 80.5 MeV calculations with the full algorithm (right), and without the INC stage (left). The various lines show the total, INC, preeq. and evaporation contributions, the exp. data have been taken from M.Trabandt et al. **PRC39** (1989) 452

Nucleon emission: thin target examples I

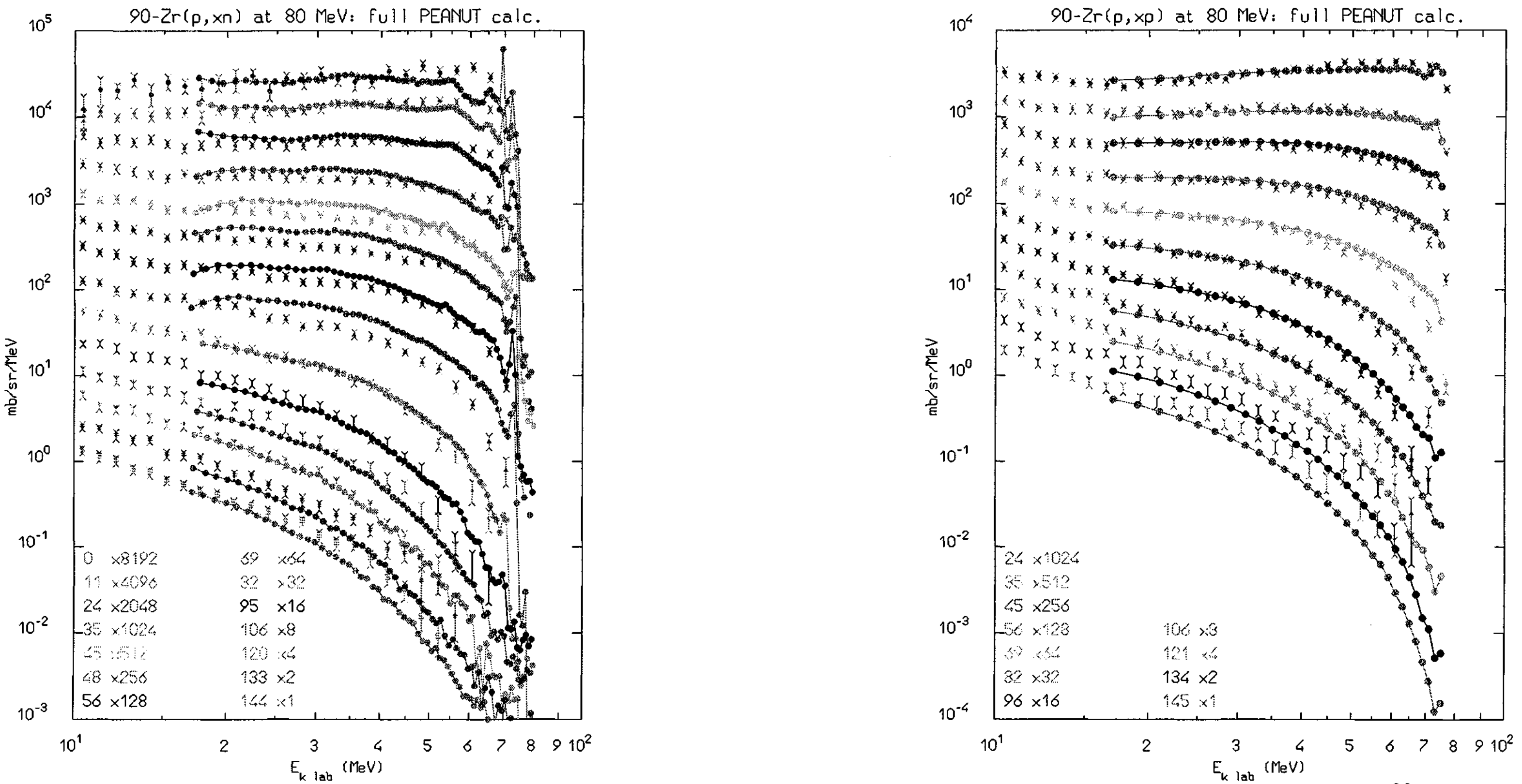

Computed (light symbols) and experimental (symbols with lines) double differential distributions for ^{90}Zr(p,xn) (left) and ^{90}Zr(p,xp) at 80.5 MeV. The exp. data have been taken from M.Trabandt et al. **PRC39** (1989) 452 and A.A. Cowley et al., **PRC43**, (1991) 678

Nucleon emission: thin target examples I

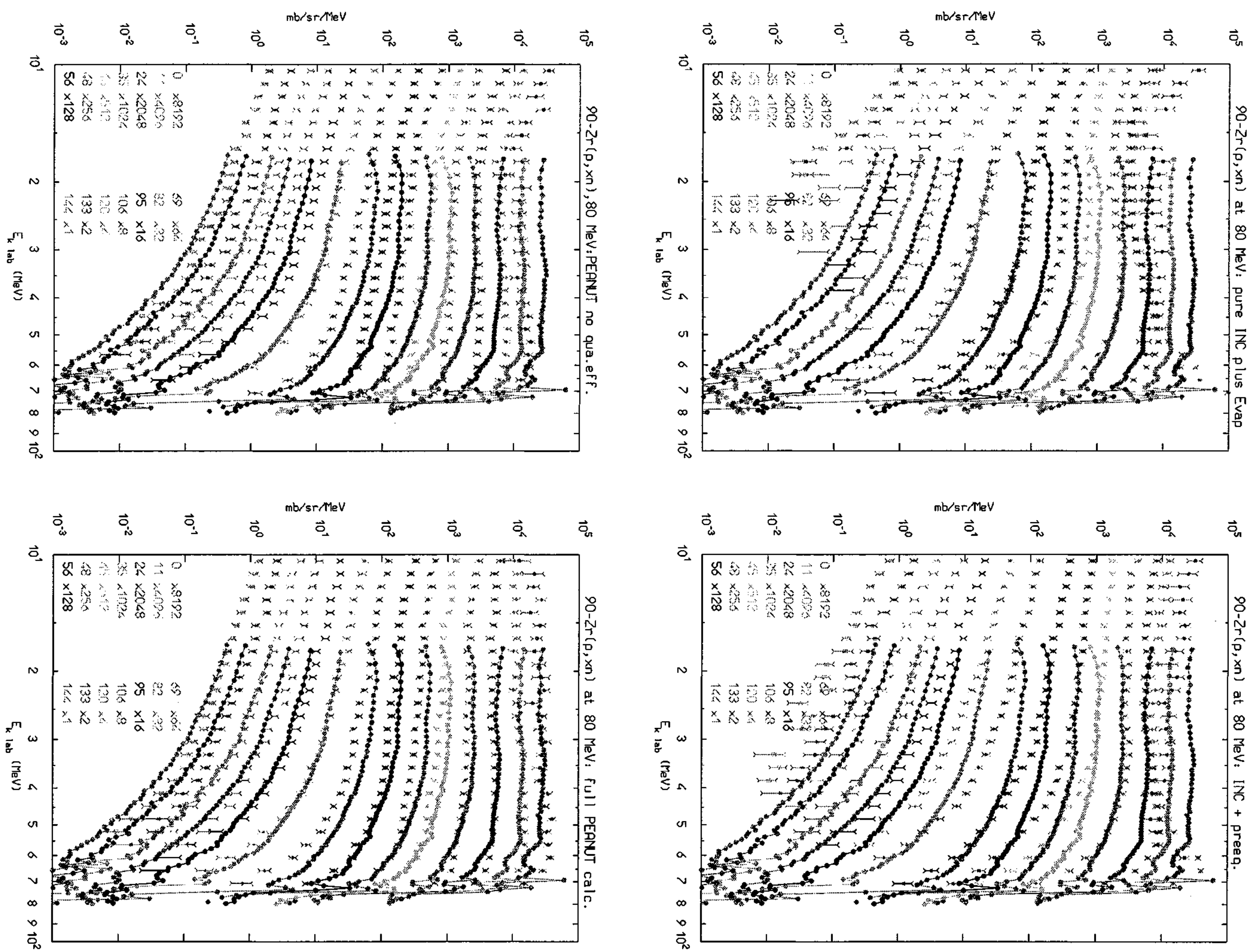

Nucleon emission: thin target examples I

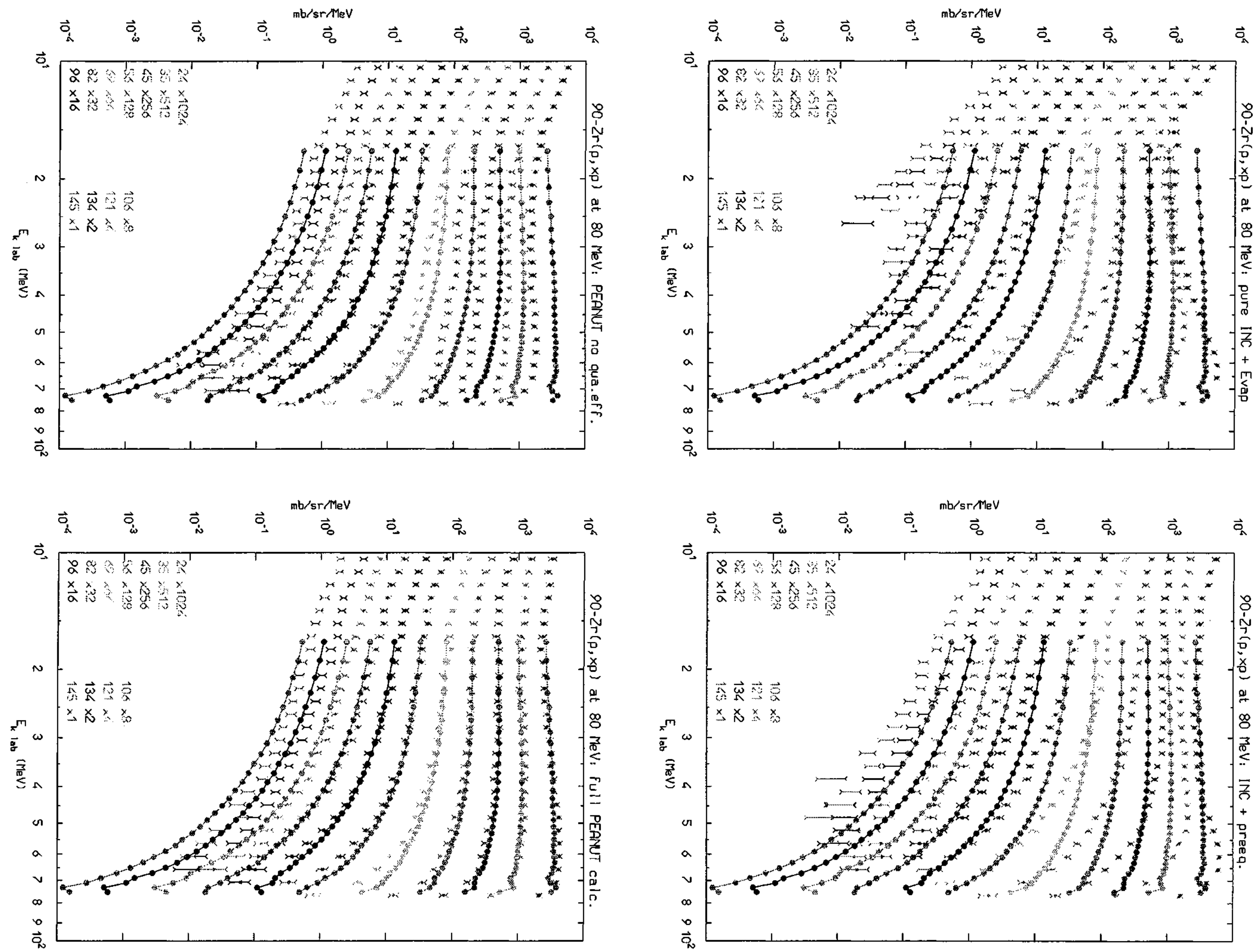

Nucleon emission: thin target examples II

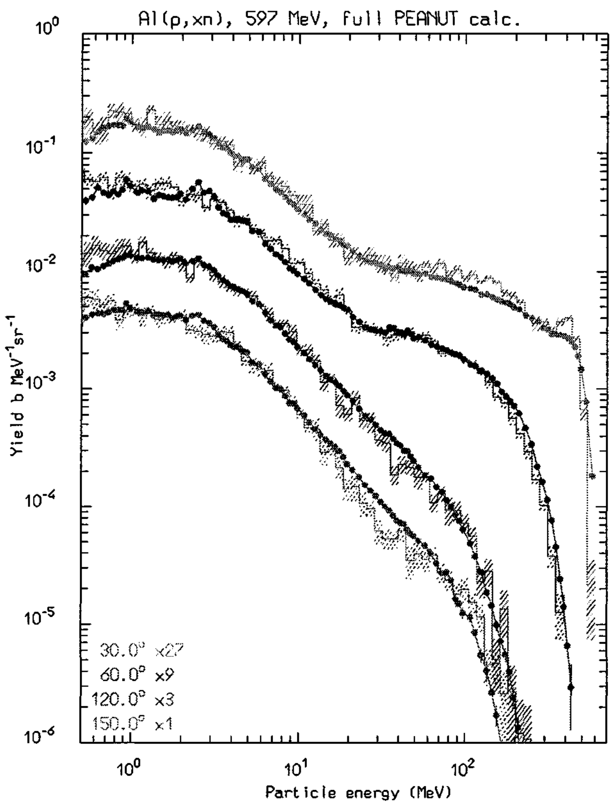

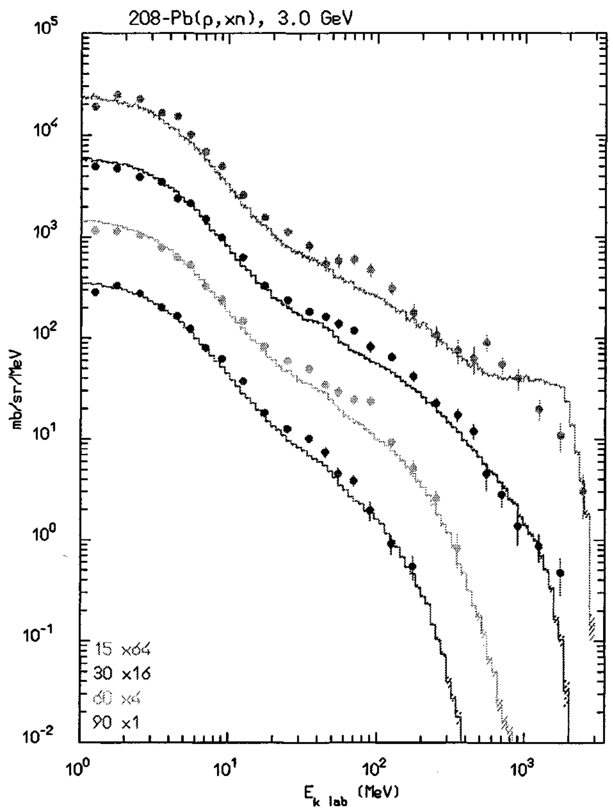

Computed (histograms) and experimental (symbols) double differential neutron distributions for Al(p,xn) (left) at 597 MeV and Pb(p,xn) at 3 GeV. The exp. data have been taken from W.B. Amian et al., Nucl. Sci. Eng. **115**, (1993) 1, and K. Ishibashi et al, Nucl. Sci. Technol. **32** (1995) 827.

Evaporation, fission and nuclear break-up

The evaporation probability for a particle of type j , mass m_j, spin $S_j \cdot \hbar$ and kinetic energy E and the total fission probability are given by
(i for initial nucleus, f for final, F at fission saddle point)

$$P_j = \frac{(2S_j+1)m_j}{\pi^2\hbar^3} \int_{V_j}^{U_i-Q_j-\Delta_f} \sigma_{\mathrm{inv}} \frac{\rho_f(U_f)}{\rho_i(U_i)} E dE$$

$$P_F = \frac{1}{2\pi\hbar} \frac{1}{\rho_i(U_i)} \int_0^{(U_i-B_F)} \rho_F(U_i - B_F - E) dE$$

- ρ's: nuclear level densities,
- Q_j: reaction Q for emitting a particle of type j,
- U: excitation energy,
- σ_{inv}: cross section for the inverse process
- V_j: (possible) Coulomb barrier for emitting a particle of type j

For low mass residuals: Fermi break-up: statistical phase-space production of multiple (excited) fragments

Excitation energy AFTER evaporation $\rightarrow$ γ emission

Latest Improvements to evaporation

- Improved state density $\rho = \exp(2\sqrt{aU})/U^{\frac{5}{4}}$
- No Maxwellian approximation for energy sampling
- γ competition in progress

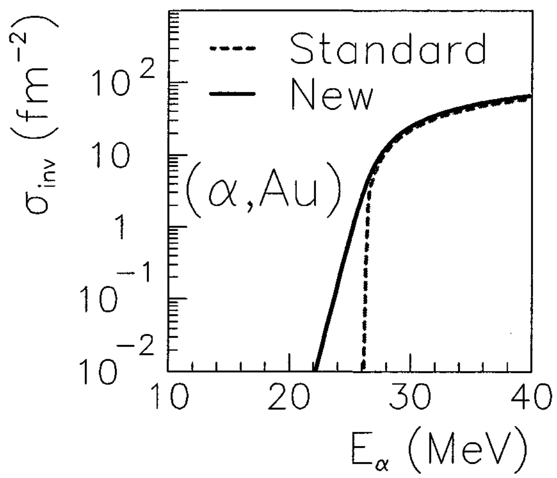

•Sub-barrier emission:

$$\sigma^x_{inv} = (R+\bar{\lambda})^2 \frac{\hbar\omega_x}{2E} \ln\left[1 + e^{\frac{2\pi(E-V_c)}{\hbar\omega_x}}\right]$$

Residual nuclei predictions: "new" vs "old" evap.

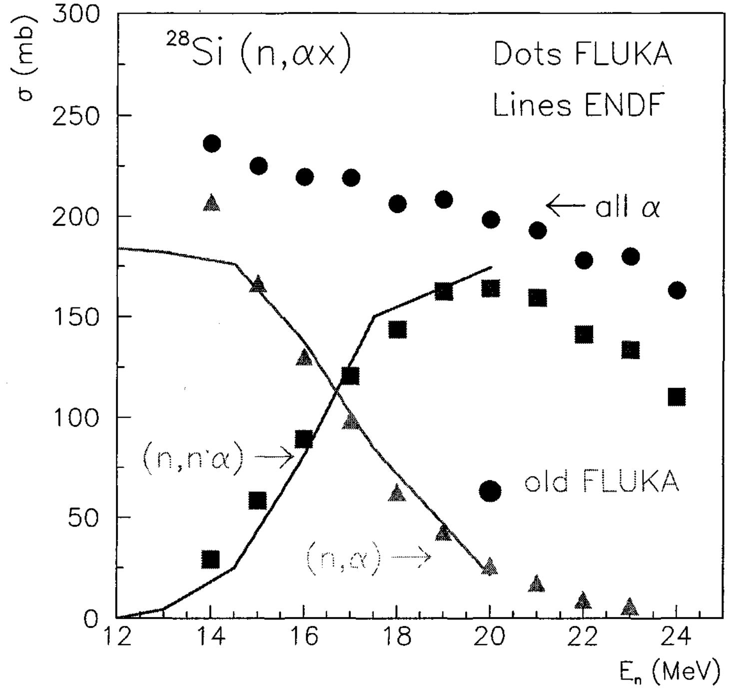

A practical case:
Si damage
α production by neutrons
compared to ENDF data

Residual nuclei

The production of residuals is the result of the last step of the nuclear reaction, thus it is influenced by ALL the previous stages

Residual mass distributions are very well reproduced

Residuals near to the compound mass are usually well reproduced

However, the production of specific isotopes may be influenced by additional problems which have little or no impact on the emitted particle spectra

- Extreme sensitivity to details of evaporation
- Nuclear structure effects
- Lack of spin-parity dependent calculations in most MonteCarlo models
- Difficulty to model fragmentation processes, that populate A<20-30 for medium/heavy target nuclei.
- Isomer production: an open question
- Interesting cross section values typically spans *four* order of magnitudes

Residual nuclei predictions: a look at the isotope table

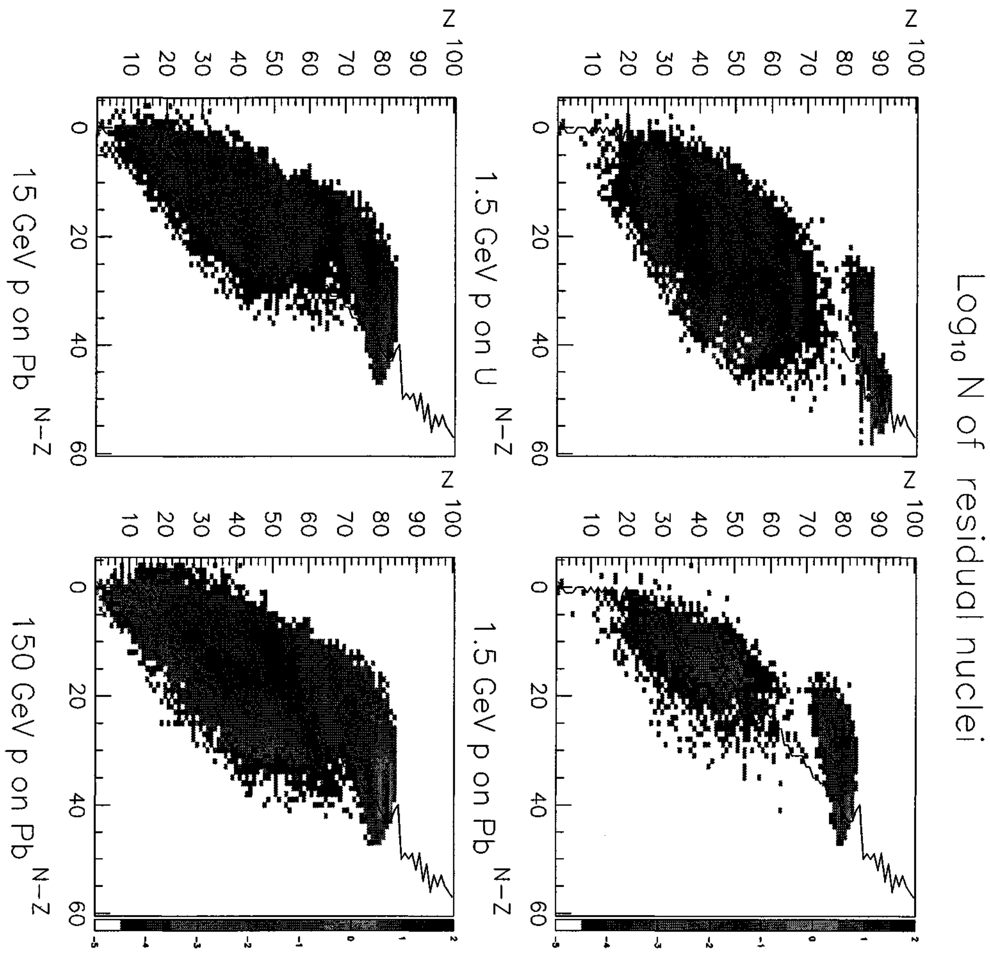

Residual nuclei: the mass distribution at high energies

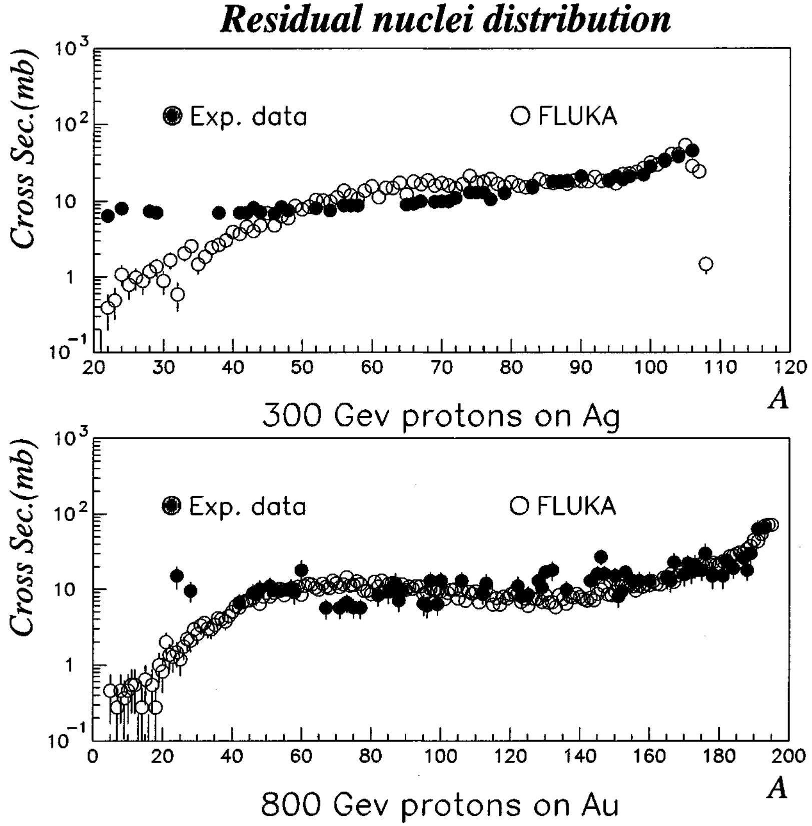

Experimental and computed residual nuclei mass distribution following for Ag(p,x)X at 300 GeV (top) and Au(p,x)X at 800 GeV (bottom).

Residual nuclei predictions: examples

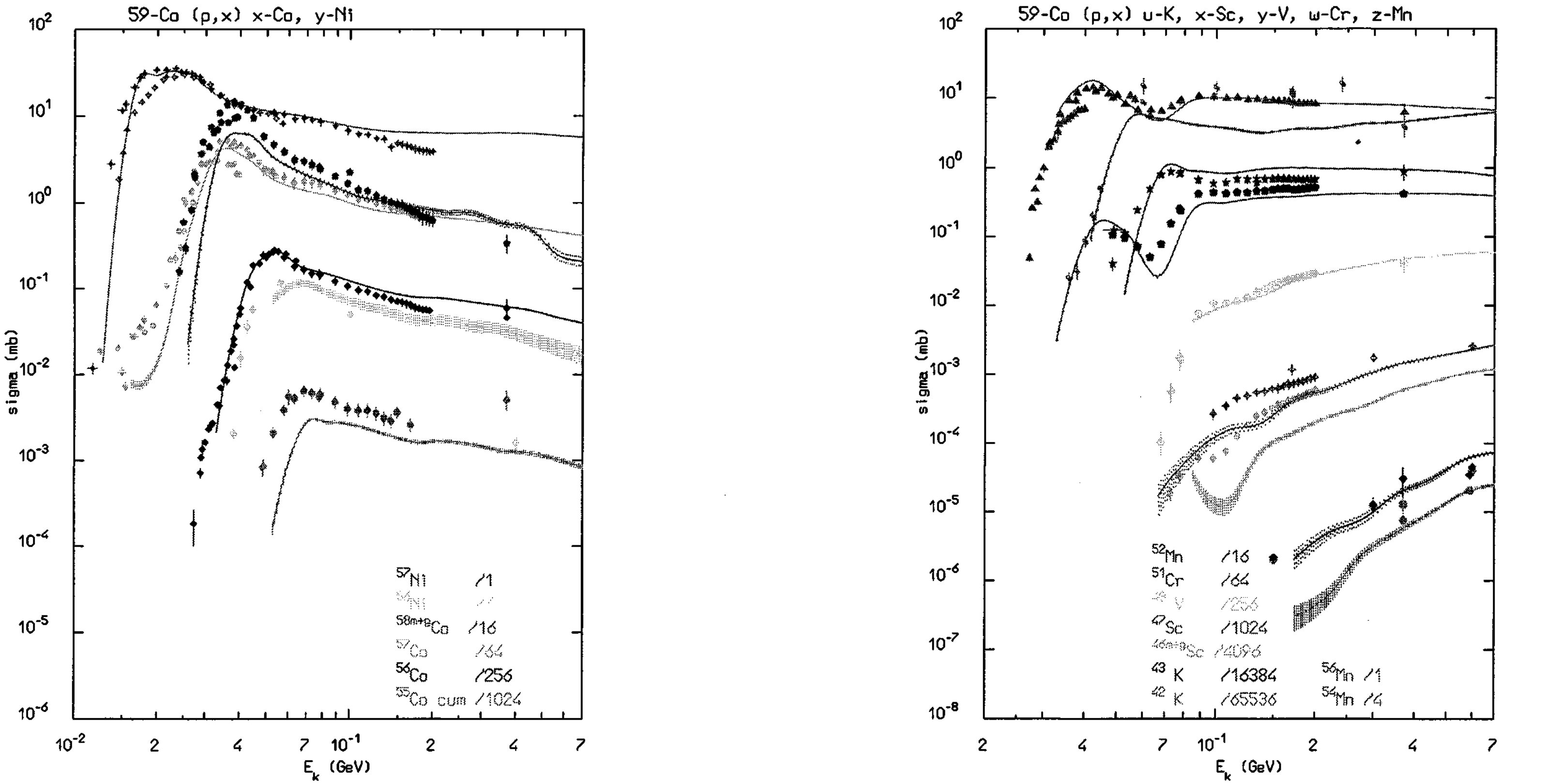

Comparison between computed and measured (A.S. Iljinov et al., Landolt-Börnstein, **Vol. 13a** (1991)) isotope production by protons on natural Cobalt

Residual nuclei predictions: examples II

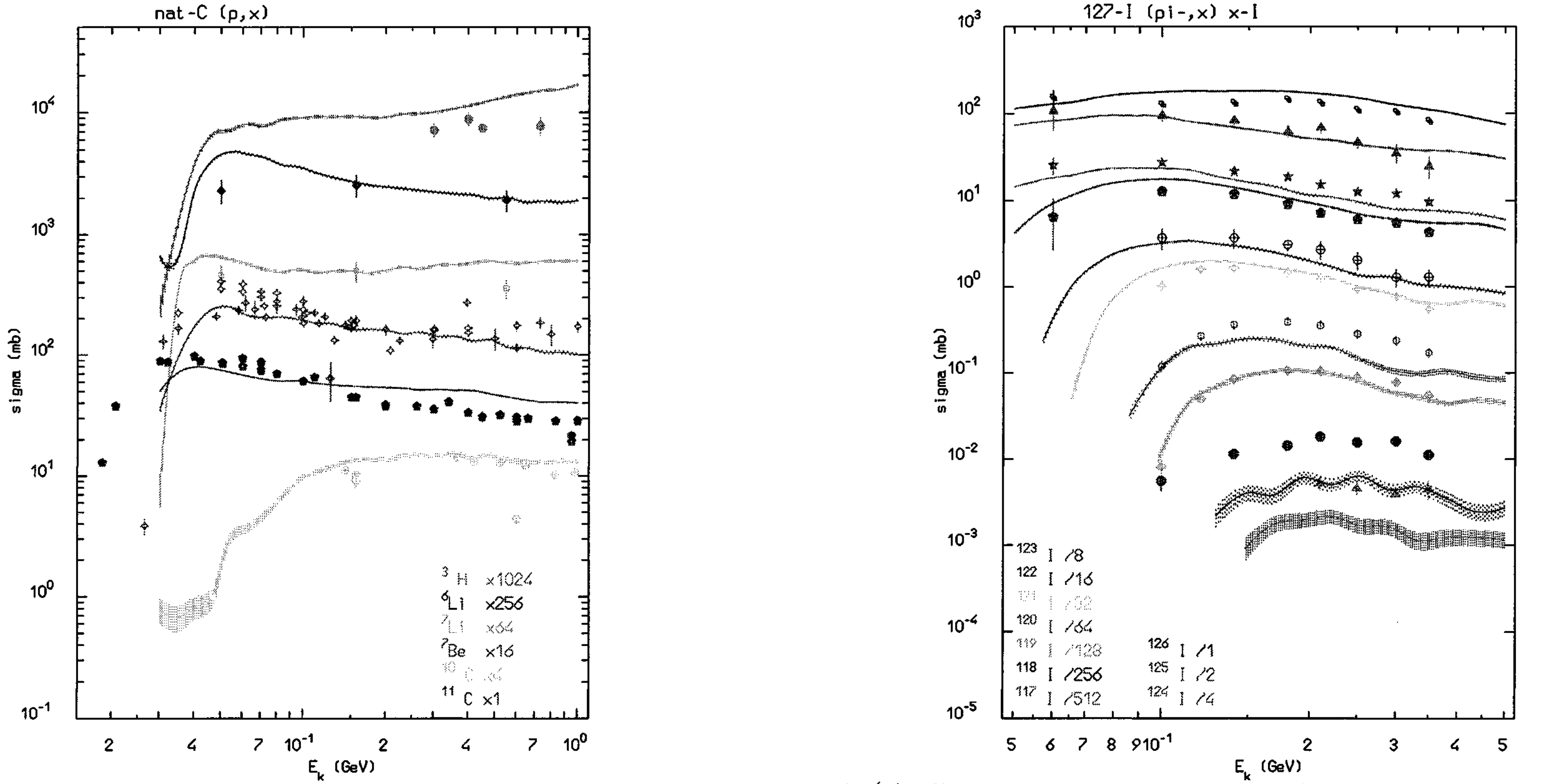

Comparison between computed and measured (A.S. Iljinov et al., Landolt-Börnstein, **Vol. 13a** (1991)) isotope production by protons on natural carbon (left) and by negative pions on Iodine (right)

An example of calculated cooldown curve

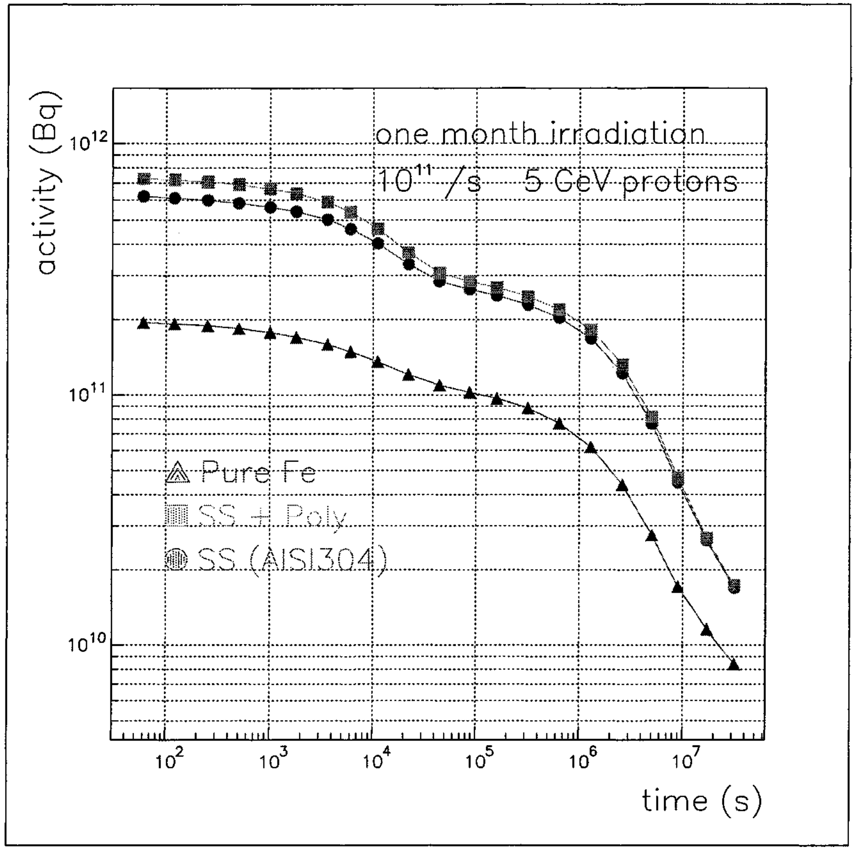

Cooling curves for residual activity for a Stainless Steel, Stainless Steel+CH_2 or Iron target (40 cm radius, 100 cm long) irradiated by 10^{11} 5 GeV protons s^{-1} for one month

Evolution of residual nuclei: SS/Iron target

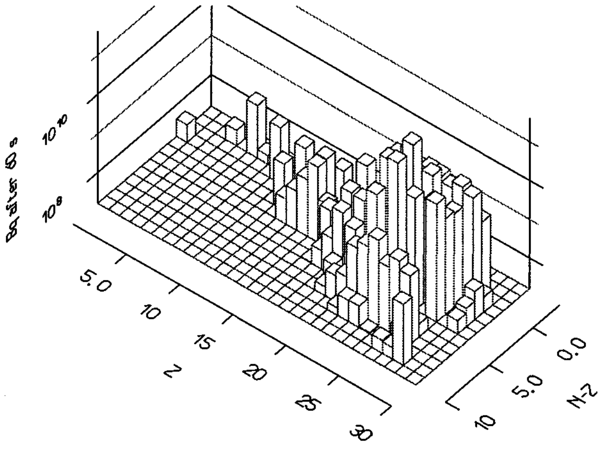

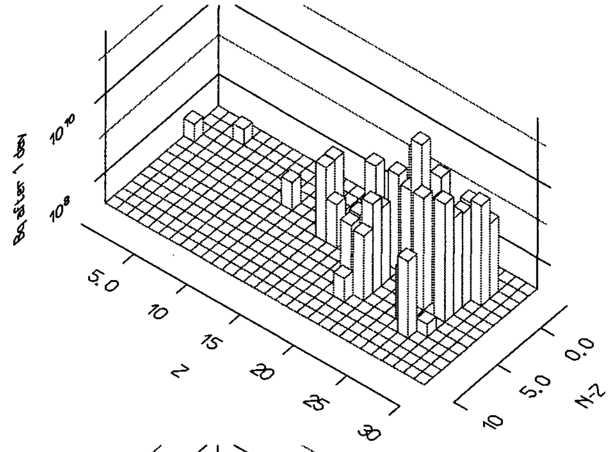

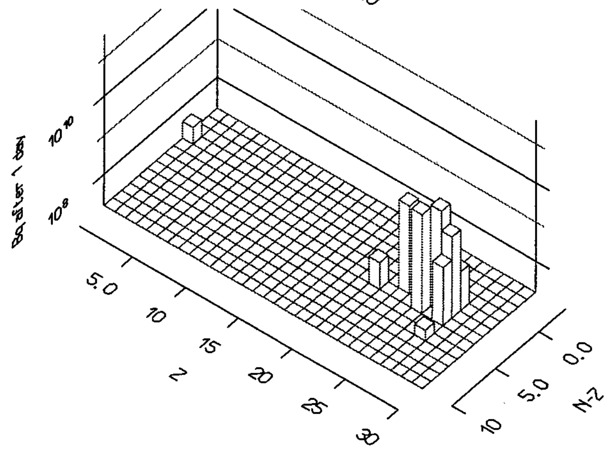

Computed residual activities (Bq) as a function of the isotope atomic number Z and neutron excess N-Z for an AISI304 target (40 cm radius and 100 cm long) irradiated by 10^{11} 5 GeV protons s^{-1} for one month: after 60 s (top left), 1 day (top right) and after 1 year (right)

LEP dismantling: a calculational nightmare

Request : demonstrate that ALL activities are below 1/10 of the 1996 European Directive limits (around 10 Bq/g) after 10 year operation

An almost unaffordable task for a MC :
Starting from an electron beam,
simulate the extremely rare photon induced nuclear interactions
with such an accuracy as to determine the residual nuclei.

EXPERIMENT: samples of different materials on LEP beam dumps.
- Irradiation time: 5 months, at about 20 cm from the beam axis
- Specific activity of the radionuclides detected in the samples were compared with FLUKA calculations
- The measured activities are so low (few Bq/g) that even the experimental measurement is difficult

Photonuclear Interactions

- Giant Resonance interaction
- Quasi-Deuteron effect
- interaction in the Delta Resonance energy region
- Vector Meson Dominance in the high energy region
- INC, preequilibrium and evaporation via the PEANUT model
- Possibility to bias the photon nuclear inelastic interaction length to enhance interaction probability

In not many other existing transport codes photonuclear reactions are simulated over the whole energy range

Photonuclear Interactions

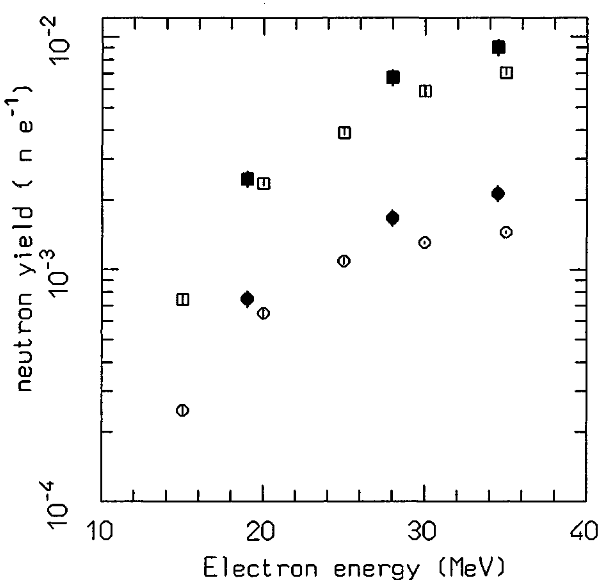

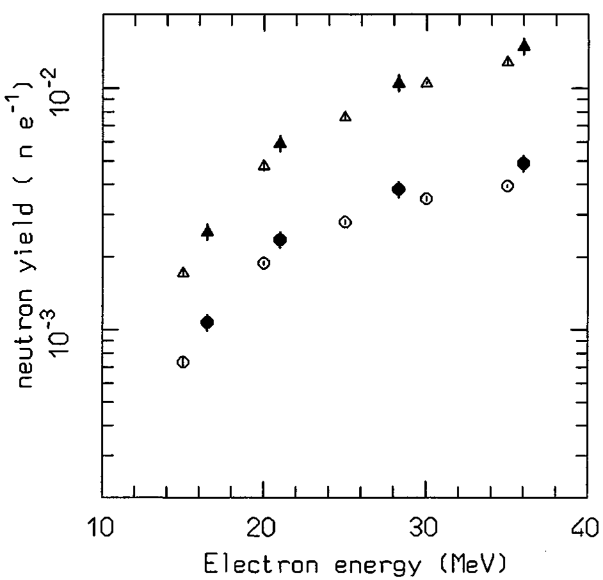

Yield of neutrons per incident electron as a function of initial electron energy. Open symbols: FLUKA, closed symbols: exp. data. Left: Pb, 1.01 (lower points) and 5.93 (upper) X_0 Right: U, 1.14 and 3.46 X_0

LEP activation: some experimental results

Radio nuclide	$T_{1/2}$	Specific Activity (Bq/g) Exp.	FLUKA	(%)	Ratio F/E
^{46}Sc	83.8 d	0.13	0.065	12	0.5
^{48}V	15.97 d	0.31	0.52	7	1.7
^{51}Cr	27.7 d	4.12	2.7	5	0.65
^{52}Mn	5.6 d	0.17	0.74	6	4.3
^{54}Mn	312.2 d	3.54	2.9	2	0.82
^{59}Fe	44.5 d	0.028	0.0088	27	0.31
^{56}Co	77.7 d	0.29	0.46	7	1.6
^{57}Co	271.8 d	1.3	1.1	4	0.85
^{58}Co	70.9 d	2.65	1.4	3	0.52
^{60}Co	5.27 y	0.18	0.085	21	0.47
^{95}Nb	34.9 d	0.038	0.013	27	0.34

Stainless Steel sample on the LEP electron dump. The exp. points have a systematic error of $\approx$20%(A.Fassò et al. CERN-TIS-99-011-RP-CF/SLAC-PUB-8214 and CERN-TIS-99-012-RP-CF/SLAC-PUB-8215)

Heavy ions

Heavy ion transport and interactions are presently under development in FLUKA:

- Ionization energy losses already implemented
  - Up-to-date effective charge parametrizations
  - Energy loss straggling according to:
    * "normal" first Born approximation
    * Charge exchange effects (dominant at low energies, ad-hoc model developed for FLUKA)
    * Mott cross section and nuclear form factors (high energies)(in progress)
- Multiple scattering already implemented
- High energy A-A interactions ($E > 5 - 10\ GeV/u$): interface to DPMJET *test phase*
- Low energy A-A interactions: extension of the PEANUT model *almost ready for tests with α's*
  The availability of exp. data on particle production in A-A collisions in the intermediate energy range will be a crucial issue in the next future

Nucleus-Nucleus interactions

- Extension of the Glauber cascade to nucleus-nucleus collisions
  - Sea-sea chains
- Generalized Intranuclear cascade for nucleons
  - Generic hadron-hadron interactions
  - Generic hadron-resonance interactions
  - Resonance-nucleon interactions
  - Nuclear mean field treatment
- Evaporation/Fission and Fermi break-up and low energies
  - Difficulties in defining the clusters prior to evaporation at low energies (target-like and projectile-like clusters definition straightforward at medium and high energies)
  - Difficulties for peripheral nucleon exchange/pickup reactions

Glauber for A-A

The Glauber quantum mechanical approach can be easily extended to nucleus-nucleus collisions (B and A nucleons for the projectile/target respectively), leading to:

$$\begin{aligned}\sigma_{BA\ abs}(s) &\equiv \sigma_{BA\ T}(s) - \sigma_{BA\ el}(s) - \sigma_{BA\ qe}(s) = \sigma_{BA\ T}(s) - \sigma_{BA\ \Sigma f}(s) = \\ &= \sigma_{BA\ r}(s) - \sigma_{BA\ qe}(s) \equiv \int \mathrm{d}^2\vec{b}\ \mu_{BA\ abs}(\vec{b}, s) \\ &= \int \mathrm{d}^2\vec{b} \int \mathrm{d}^3\vec{w}\ |\Psi_{iB}(\vec{w})|^2 \int \mathrm{d}^3\vec{u}\ |\Psi_{iA}(\vec{u})|^2 \\ &\cdot \left\{1 - \prod_{k=1}^{B}\prod_{j=1}^{A}\left\{1 - \left[1 - |S_{hN}(\vec{b} - \vec{r}_{j\perp} + \vec{d}_{k\perp}, s)|^2\right]\right\}\right\}\end{aligned}$$

The Glauber formalism allows to compute the probability of having N_B projectile and N_A target nucleons hit. The average numbers of projectile/target as well as total nucleons hit are given by:

$$< N_B >= \frac{B\sigma_{NAabs}}{\sigma_{BA\ abs}}, \quad < N_A >= \frac{A\sigma_{NBabs}}{\sigma_{BA\ abs}}, \quad < N_{AB\ hit} >= \frac{AB\sigma_{r\ NN}}{\sigma_{BA\ abs}}$$

Cascading/evaporation in A-A collisions (ZPC71,75 (1996))

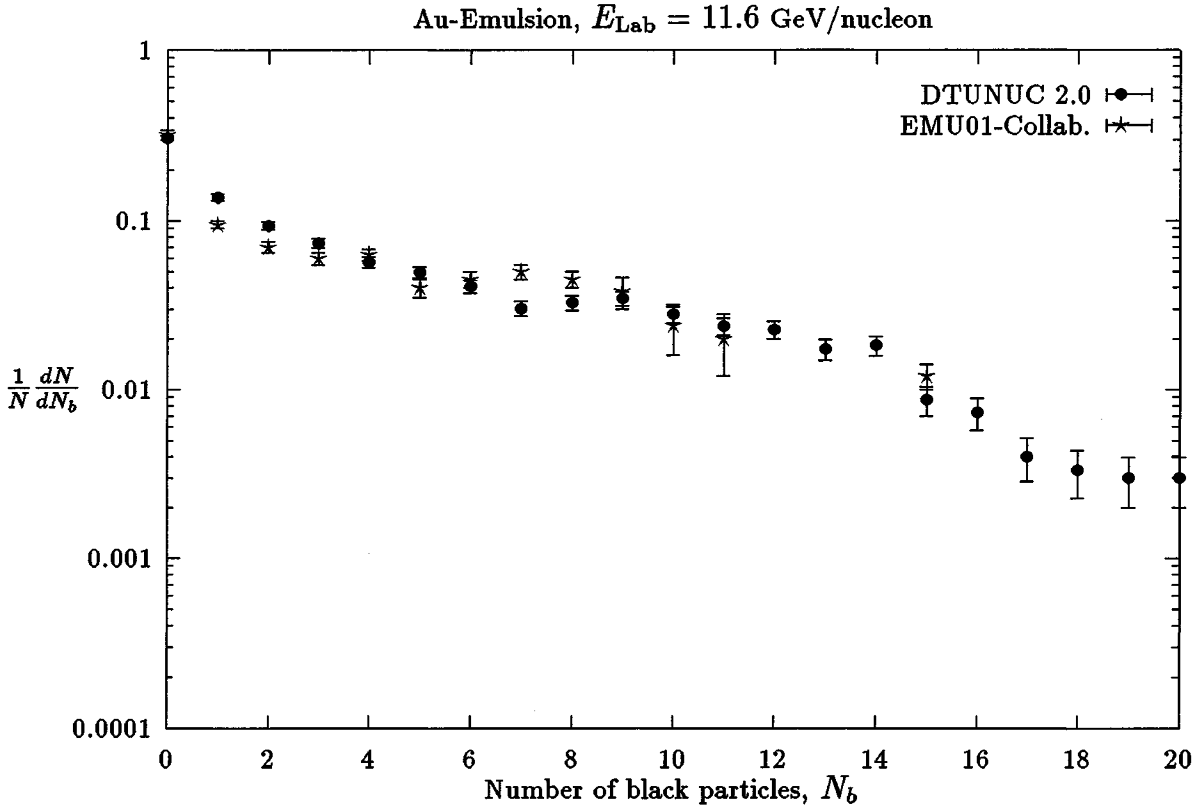

Black particle multiplicity distributions in gold-emulsion interactions compared with exp. data (ZPC65, 421 (1995))

Neutrino interactions in PEANUT: *NUX-FLUKA*

Authors: A. Ferrari, A. Rubbia, P.R. Sala

Quasielastic event generator built-in

RES and DIS: νN interaction via *NUX* (A.Rubbia, originally for NOMAD)

Nuclear effects from PEANUT

Comparison with NOMAD data A. Bueno, A. Rubbia, ETH Zurich

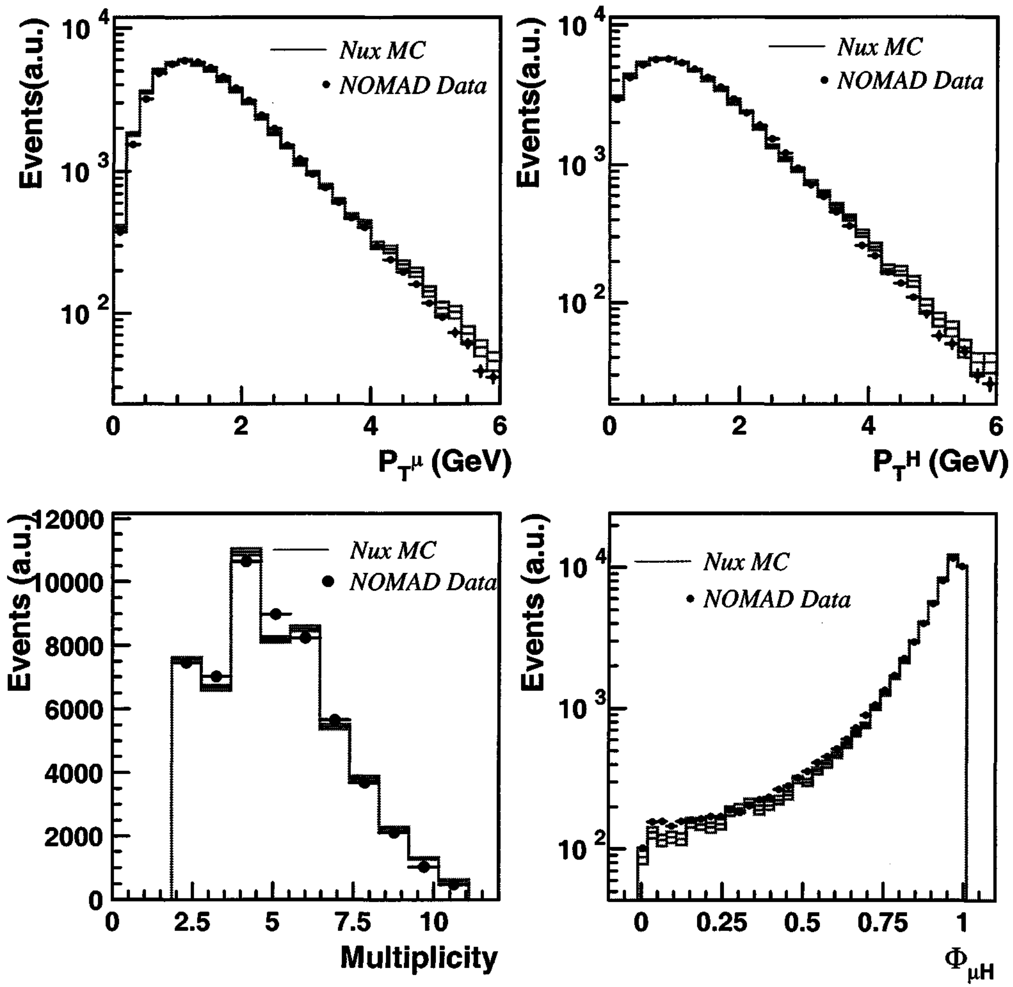

Thick target neutron production: examples

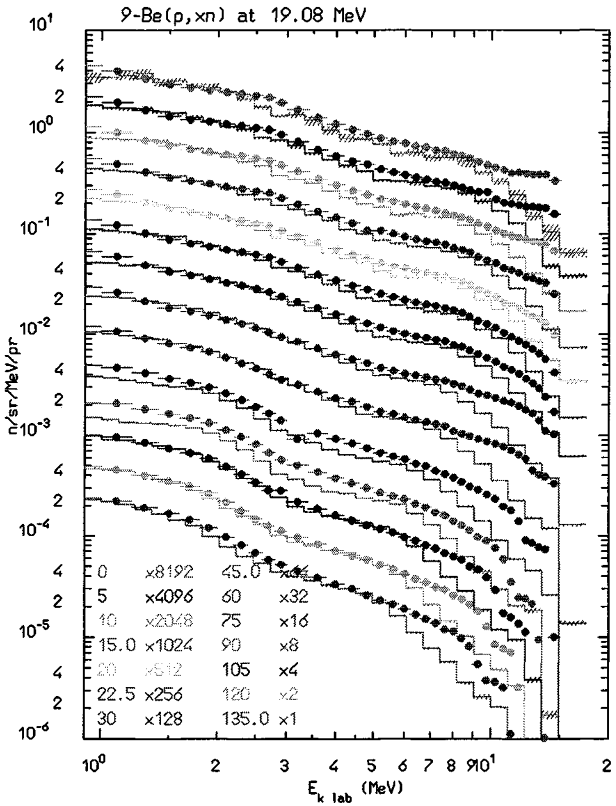

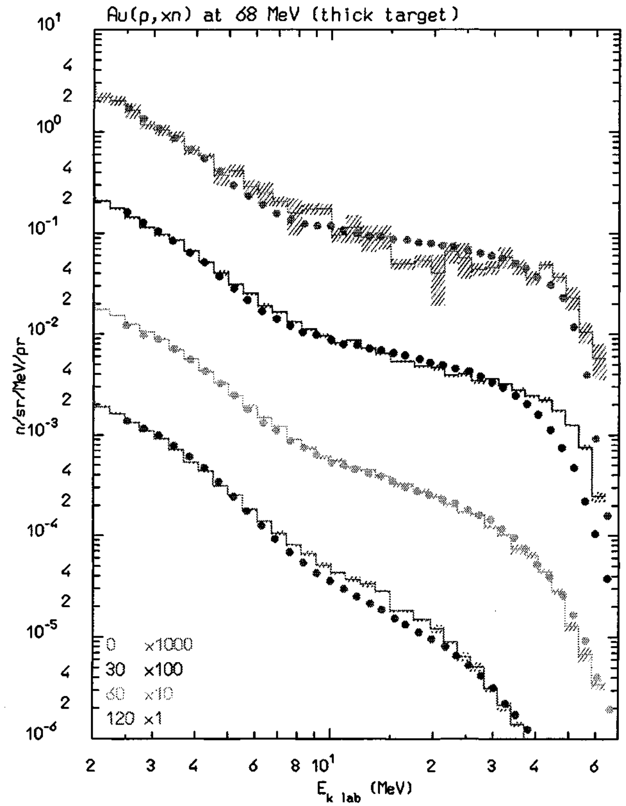

Simulated (dashed histogram) and experimental (symbols) neutron double differential distributions out of stopping length targets for 19.08 MeV protons on beryllium (left, H.J. Brede et. al., **NIMA274** (1989) 332) and 68 MeV protons on gold (right, S. Meigo et al., NDST97)

Thick target neutron production: examples II

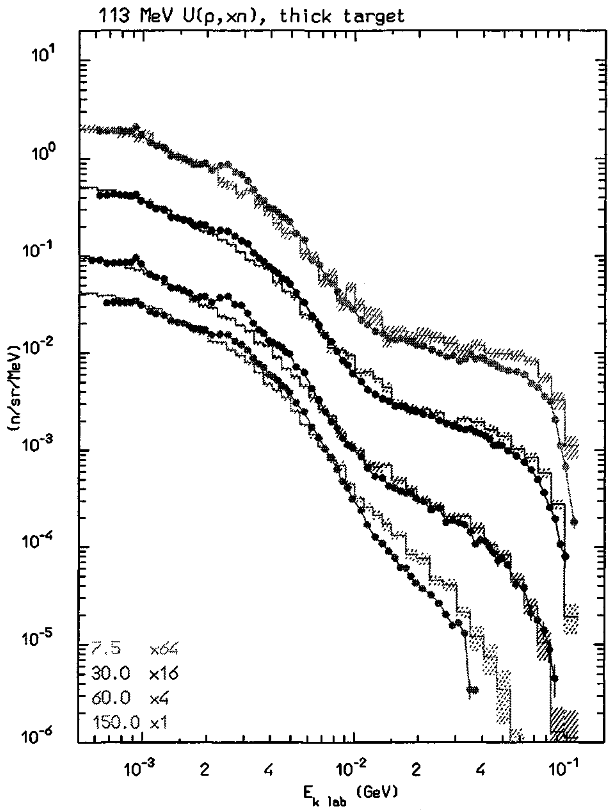

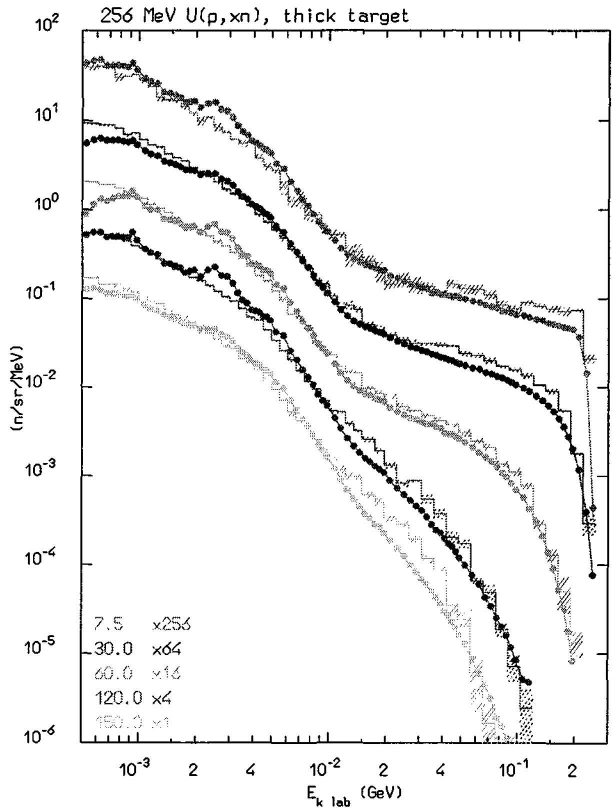

Simulated (dashed histogram) and experimental (symbols) neutron double differential distributions out of stopping length targets for 113 (left, M.M. Meier et al., Nucl. Sci. Eng. **110**, (1992) 299) and 256 MeV protons on uranium (right, M.M. Meier et al., Nucl. Sci. Eng. **102**, (1989) 310)

Thick target neutron production: examples III

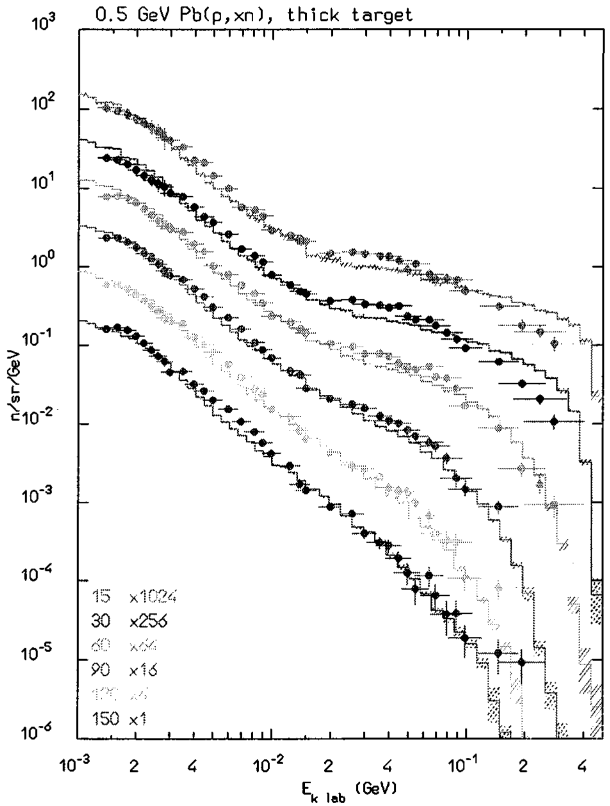

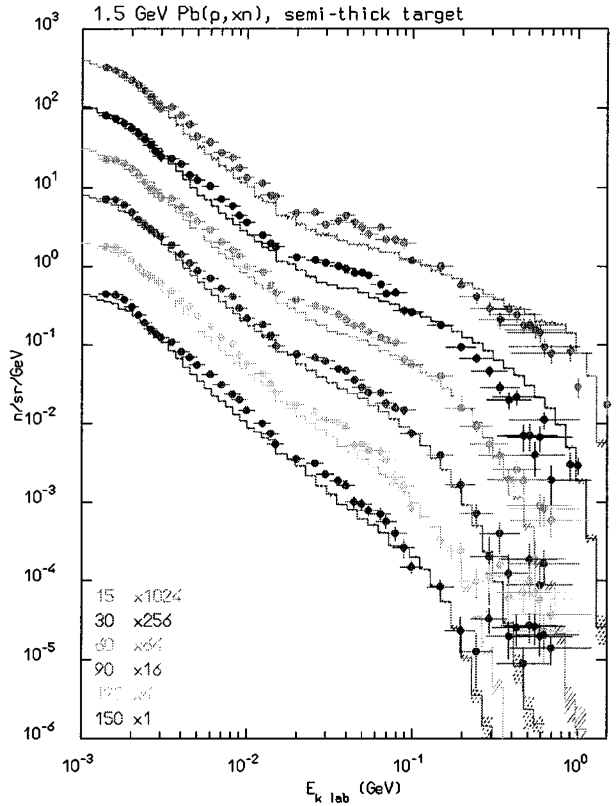

Simulated (dashed histogram) and experimental (symbols) neutron double differential distributions out of (semi)stopping length targets for 500 (left) and 1500 MeV protons on lead (right). Exp. data from S. Meigo et al., JAERI-Conf 95-008, (1995), 213

Neutron transport below 20 MeV

- ENEA multigroup cross-sections: 72 groups, $\approx$100 elements/isotopes
- gamma-ray generation,different temperatures, Doppler broadening, self-shielding.
- Transport: standard multigroup transport with photon and fission neutron generation.
- Detailed kinematics and recoil transport for elastic and inelastic scattering on hydrogen nuclei.
- Photons transported with the EMF package
- Kerma factors to calculate energy deposition
- residual nuclei production

Charged particle transport

Ionization energy losses (below δ threshold)

Latest recommended values of ionization potential and density effect parameters implemented (Sternheimer, Berger & Seltzer) (can be overridden on user's request)
Special treatment of positron dE/dx (Kim et al. 1986)
A new general approach to ionization fluctuations

Multiple coulomb scattering

path length correction, lateral displacement, angle correlation
Soft approach to boundaries
Single scattering available, automatic if needed
Screening and spin-relativistic correction
Fully coupled to magnetic field transport

The OPTIS beam at PSI

Context : PSI therapy unit : 72 MeV proton beam, fully-modulated
Goal: Full understanding of its physical and radiobiological features
Emphasis: relationship between dosimetrical quantities and biological effects
Assumption: clustered DNA damage is an estimator for cell inactivation

Solution :Combined physical-biophysical simulation of the OPTIS beam

The input data used in the simulation were fixed a priori on the basis of informations provided by PSI.

No free parameter was introduced and no a posteriori fit to experimental data was performed.

The results were directly compared with the measurements of the physical dose and with experimental data on cell survival [3].

[3] M. Biaggi et al., NIMB **159** (1999) 89

The OPTIS beam at PSI II

Simulation approach:

- Full simulation of all beam line elements including the rotating beam shapers used for generating the Spread Out Bragg Peak (SOBP) and the actual beam emittance (technical part)
- Simulation of primary and secondary radiation fields associated with the proton beam and their interactions with the phantom tissue (physical part)
- "Weighting" of each track segment with the particle/energy dependent probability of inducing complex DNA lesions [4] (CL) as obtained from track structure simulations of DNA damage using the MOCA code [5] for the time being and the PARTRAC code [6] in the future (biophysical part)

---

[4] Operatively defined as two or more single-strand breaks on each DNA strand within 30 base pairs
[5] A. Ottolenghi, M. Merzagora, H.G. Paretzke, Radiat. Environ. Biophysics, **36**, (1997) 97
[6] W. Friedland et al., Radiat. Environ Biophys, **38** (1999) 39

Absorbed Dose and its components

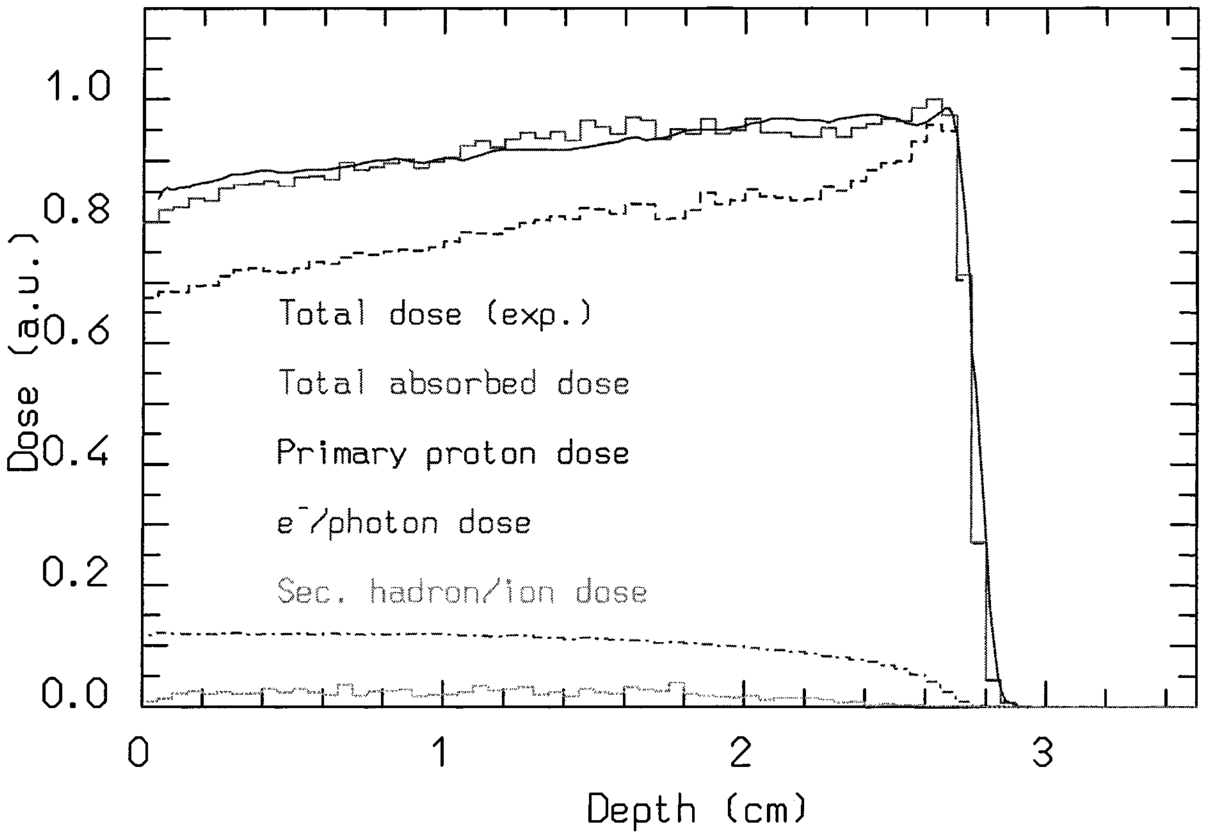

Measured (red) and calculated (green) depth-dose curves in perspex of 72 MeV modulated proton beam. The calculated dose is split into the contribution of primary protons (blue), electrons and photons (purple) and secondary hadrons including ions (light blue).

The Clustered DNA damage

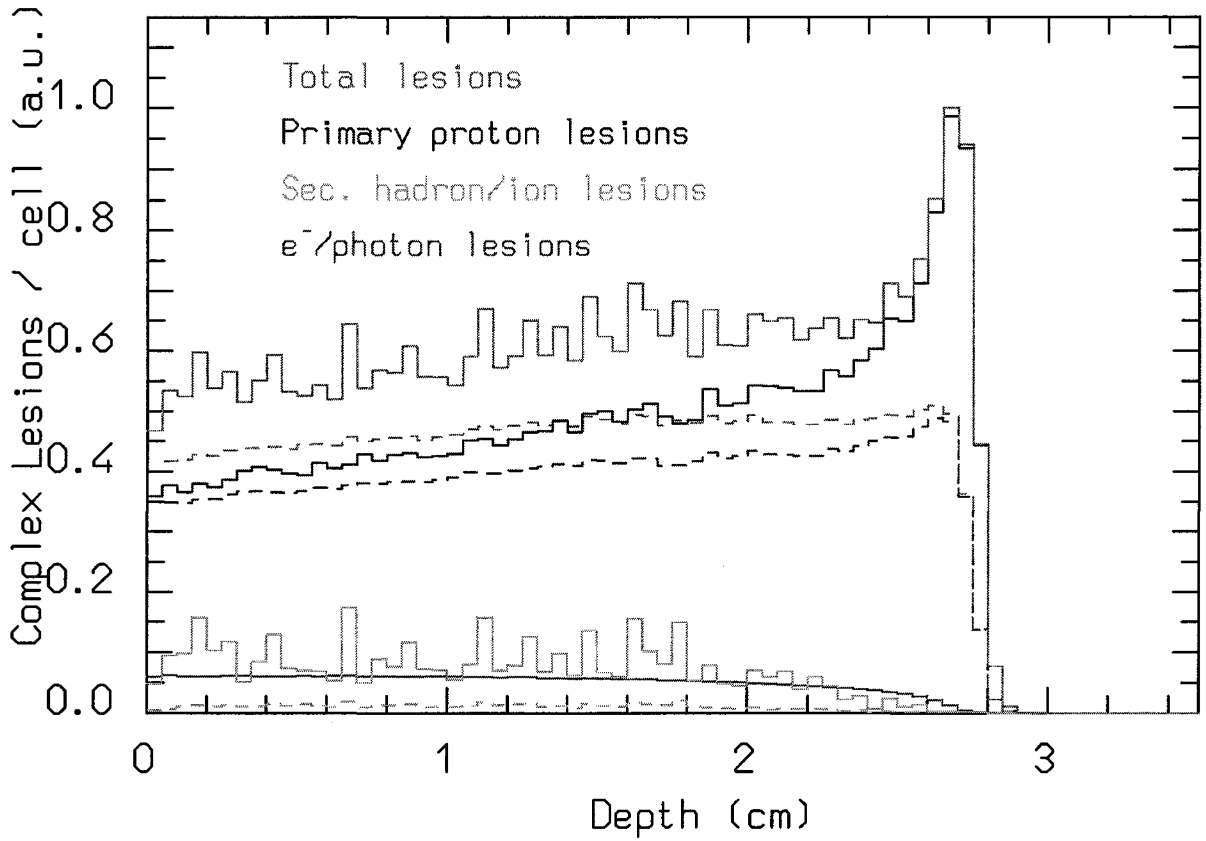

Calculated relative number of complex lesions per cell. For each component the upper (full) line represents the yield of complex lesions/cell, whereas the lower curve (dashed) represents the yield that one would obtain assuming an effectiveness equal to that of x-rays.

OPTIS: relative effectivness of protons wrt x-rays

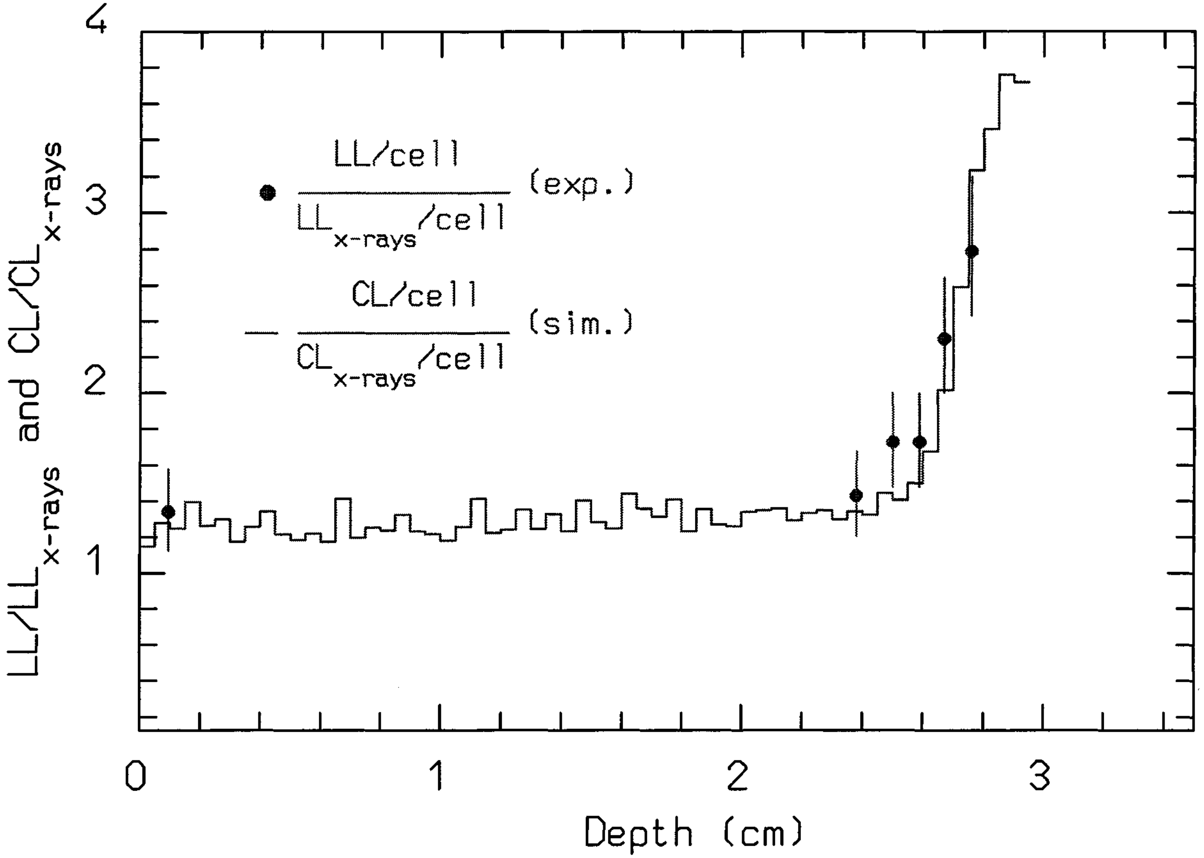

Simulation (blue curve): ratio between DNA complex lesions/cell (CL/cell) after irradiation with 2 Gy in the 72 MeV proton beam and with x-rays. Experimental data (red points): ratio between lethal lesions/cell (LL/cell) in V79 cells after irradiation with 2 Gy in the 72 MeV proton beam and with x-rays.

The ingredients and the recipe

1. Primary Cosmic Ray Spectra
2. Atmosphere description — 51 concentric shells of a mixture of N,O,Ar
3. Particle transport and decay
4. Hadronic interactions — G. Battistoni et al now2000
5. Geomagnetic effects — Dipole or map, applied a posteriori
6. Geometry :3D/1D — G. Battistoni et al.,Astropart. Phys 12 (2000) 315
7. Minor local corrections
8. ν interactions — NUX-FLUKA

Standard Calculations: HKKM [7] Bartol [8]

[7] M.Honda et al. , Phys Rev.D52 (1995) 4985
[8] V. Agrawal et al., Phys Rev.D53 (1996) 1314

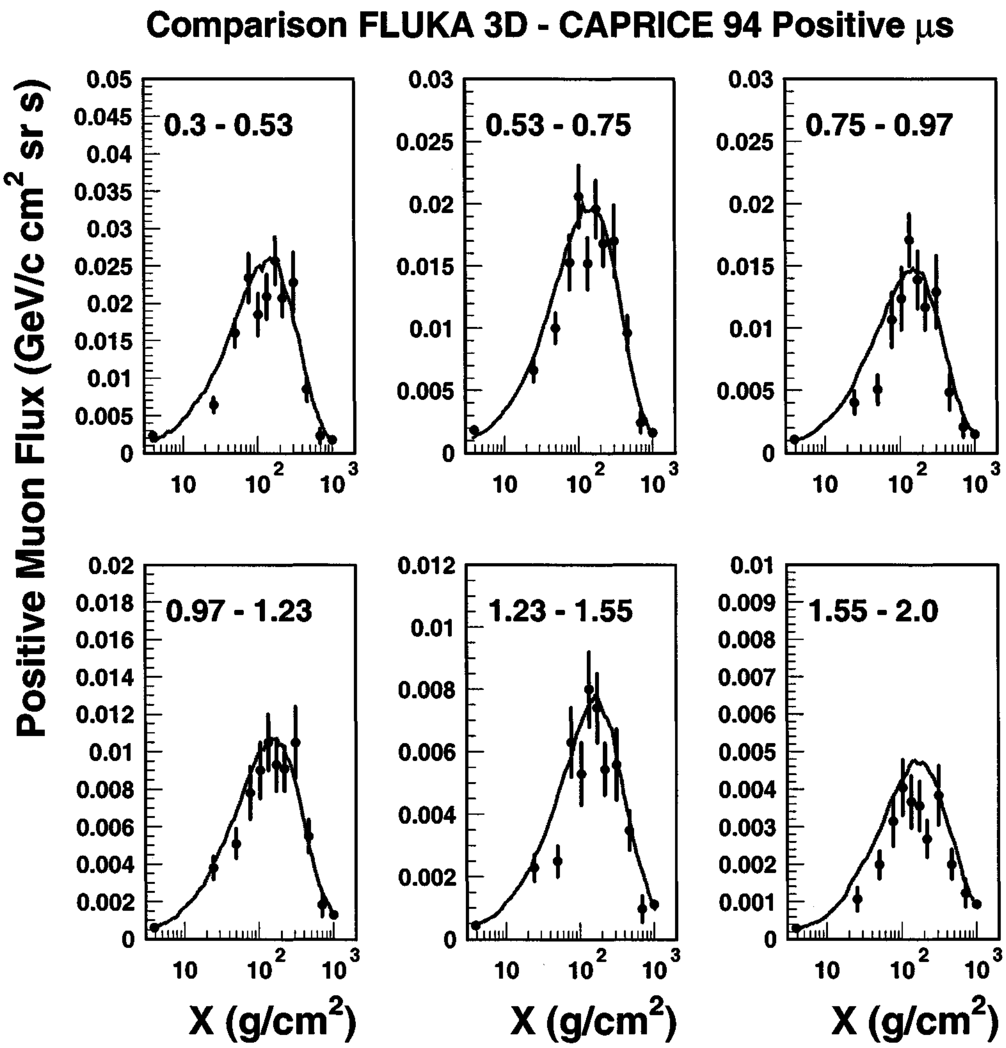
Comparison FLUKA 3D - CAPRICE 94 Positive μs
Positive Muon Flux (GeV/c cm² sr s)
0.3 - 0.53
0.53 - 0.75
0.75 - 0.97
0.97 - 1.23
1.23 - 1.55
1.55 - 2.0
X (g/cm²)
X (g/cm²)
X (g/cm²)

Radiation Field at Aircraft altitudes

S. Roesler, W. Heinrich, H. Schraube, SLAC-PUB-8968
Courtesy of S. Roesler

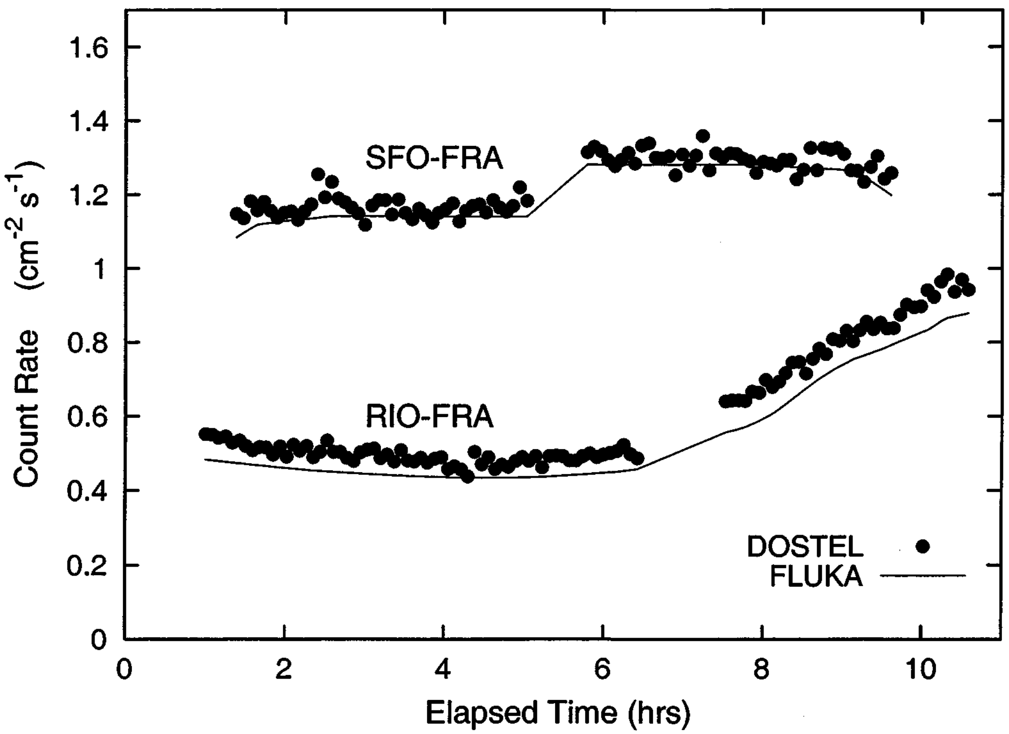

Ionizing radiation as a function of elapsed time after take-off, on commercial flights from San Francisco and Rio de Janeiro to Frankfurt

Data from R. Beaujean, J. Kopp and G. Reitz, Rad. Prot. Dosim 85,287 (1999)

Radiation Field at Aircraft altitudes

S. Roesler, W. Heinrich, H. Schraube, SLAC-PUB-8968

Courtesy of S. Roesler

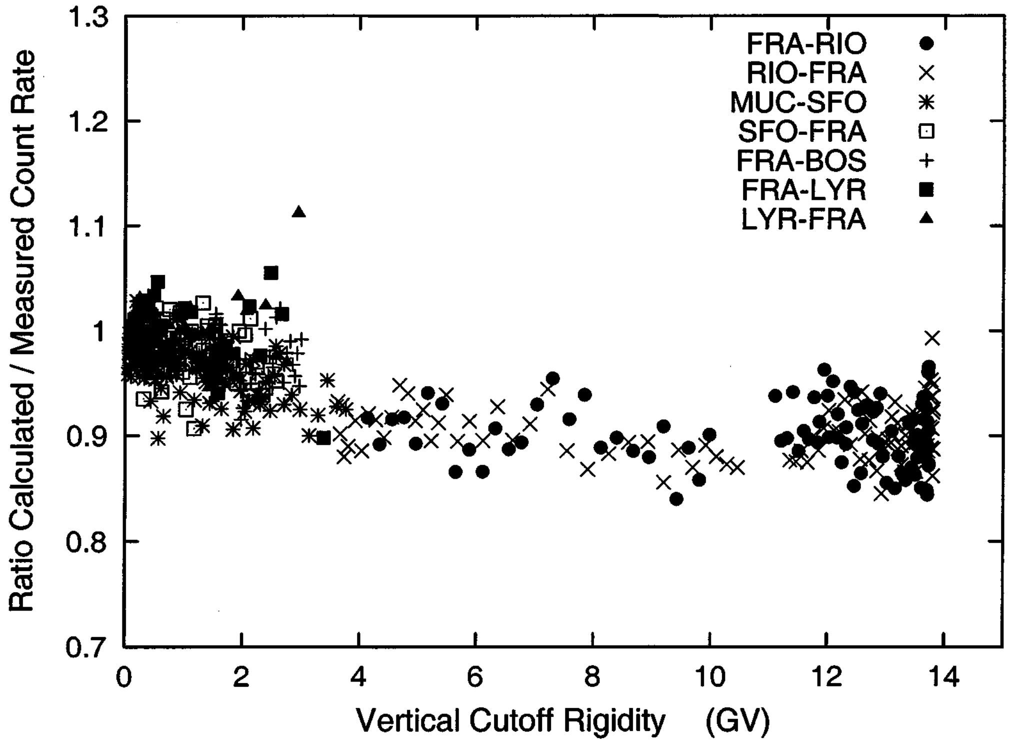

Ionizing radiation as function of vertical rigidity cutoff on commercial flights.

Data from R. Beaujean, J. Kopp and G. Reitz, Rad. Prot. Dosim 85,287 (1999)

S. Roesler, W. Heinrich, H. Schraube, SLAC-PUB-8968 Courtesy of S. Roesler

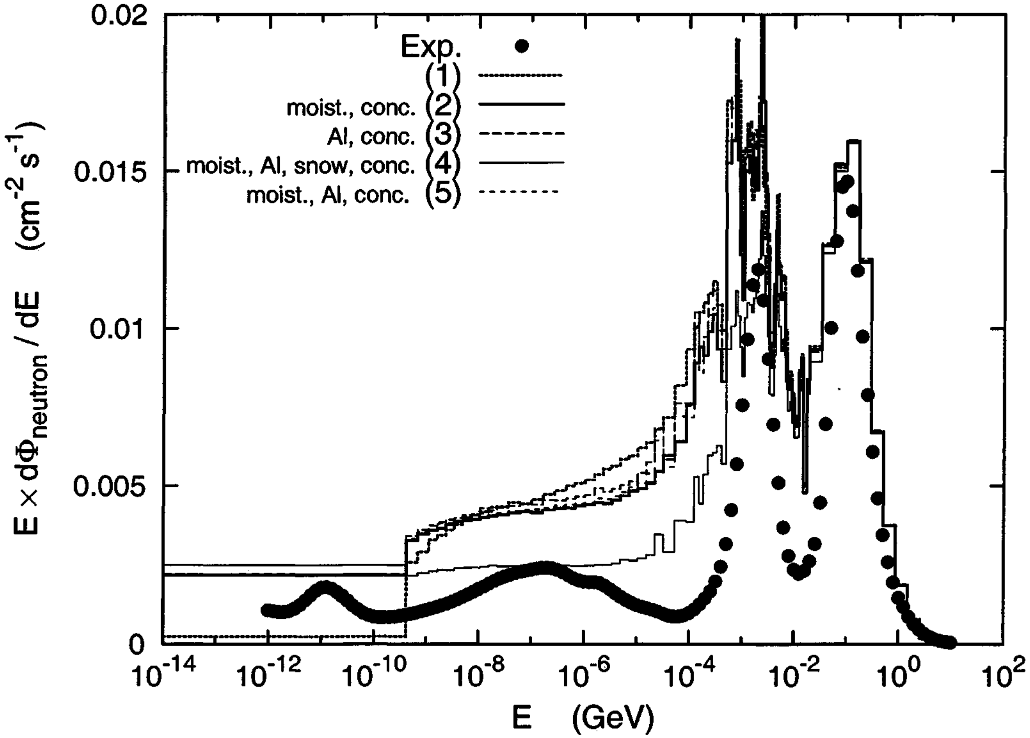

Ground-level neutron spectra at the Schneefernerhaus (2660 m a.s.l). Calculations with different humidity and soil

Data from H. Schraube et al., Rad. Prot. Dosim. 86,309(1999) and Rad. Prot. Dosim. 70,405 (1997)

Doses to commercial flight crews (M.Pelliccioni et al, work in progress)

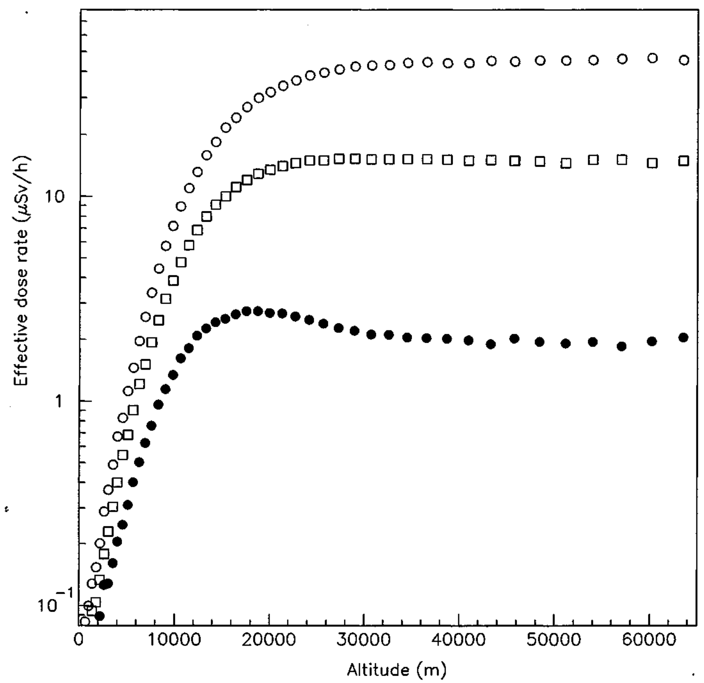

Calculated effective dose as a function of altitude for a vertical rigidity cutoff of 0.4 GV at solar minimum (open circles), and at solar maximum (open squares), and for a cutoff of 17.6 GV (black circles)

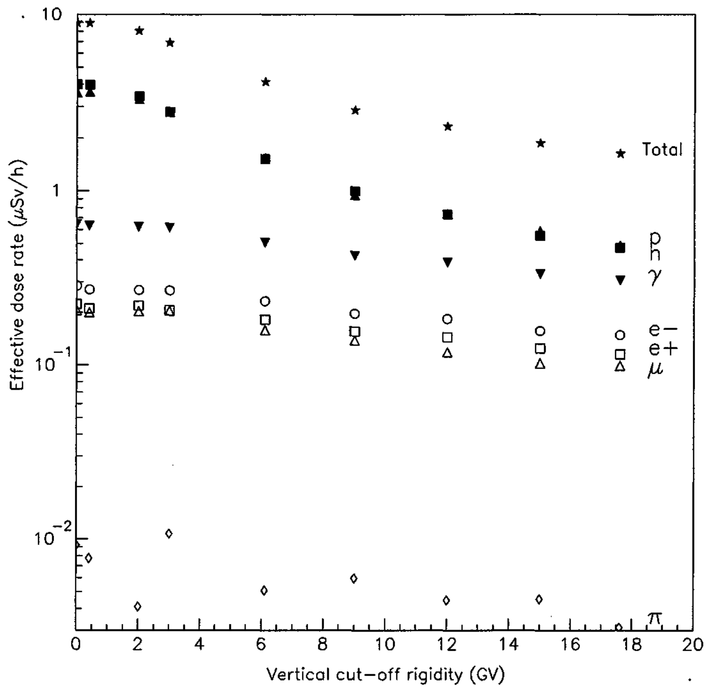

Contributions of various radiation components to the effective dose rate as a function of the vertical cut-off rigidity at solar minimum, and for an altitude of 10580 m

Doses to commercial flight crews (M.Pellicccioni et al, work in progress)

Doses to commercial flight crews (M.Pelliccioni et al, work in progress)

A. Ferrari, M. Pelliccioni and T. Rancati , Rad. Prot. Dos. 2001
A comparison of calculated ambient dose equivalent rates with in–flight measurements for different altitudes and geomagnetic latitudes (μSv/h).

B_m (°)	Vertical cut–off (GV)	FL 310 (9450 m)	FL 330 (10060 m)	FL 350 (10670 m)	FL 370 (11280 m)	FL 390 (11890 m)
–25.98	6.1	2.4 2.7	2.7 3.0	3.1 3.5	3.4 3.8	3.7 4.1
– 22.43	12.0	2.2 1.6	2.5 1.8	2.8 2.0	3.2 2.4	3.5 2.5
– 9.42	12.0	1.7 1.6	1.9 1.8	2.3 2.0	2.6 2.4	2.9 2.5
– 0.18	17.6	1.5 1.1	1.8 1.3	2.0 1.4	2.2 1.5	2.5 1.6
4.18	15.0	1.5 1.3	1.7 1.5	1.8 1.7	2.1 1.9	2.4 2.0
11.27	15.0	1.4 1.3	1.7 1.5	1.7 1.7	1.9 1.9	2.3 2.0
15.23	15.0	1.5 1.3	1.7 1.5	1.9 1.7	1.9 1.9	2.3 2.0
17.53	15.0	1.5 1.3	1.6 1.5	2.0 1.7	2.0 1.9	2.3 2.0
29.67	9.0	2.0 2.0	2.4 2.2	2.3 2.5	2.5 2.8	3.2 3.0
33.40	9.0	2.2 2.0	2.6 2.2	2.7 2.5	2.7 2.8	3.9 3.0
33.49	9.0	2.2 2.0	2.6 2.2	2.7 2.5	2.7 2.8	3.9 3.0
34.64	6.1	2.6 2.7	2.7 3.0	2.7 3.5	2.7 3.8	4.0 4.1
45.57	3.0	3.8 4.4	4.2 4.9	4.1 5.6	5.3 6.5	6.7 7.2
65.49	0.4	4.5 5.5	5.4 6.4	6.2 7.4	7.3 8.5	8.2 9.5

Differences < 20 % for 78% of data, <34 % for all

Data (upper lines) : U.J. Schrewe, NIM A422, 621 (1999)

The CERN reference radiation facility – CERF

- A reference radiation facility (called CERF) for the calibration and intercomparison of dosimetric devices in high energy stray radiation fields is available at CERN since 1993, on the H6 beam line in the North Area.
- Hadron beams with momentum of either 120 or 205 GeV/c are stopped in a copper target, which can be installed in two different positions. On top and on side of these two positions, the secondary particles produced in the target are filtered by a shielding made up of either concrete or iron.
- The facility is partially supported by the European Commission in the framework of a research program for the assessment of radiation exposure at civil flight altitudes.
- The composition of the CERF field is accurately known by means both of FLUKA calculations and measurements with several instruments which nicely agree each other. Some examples of comparisons of computed vs measured data are presented in the following.

Neutron detector calibration

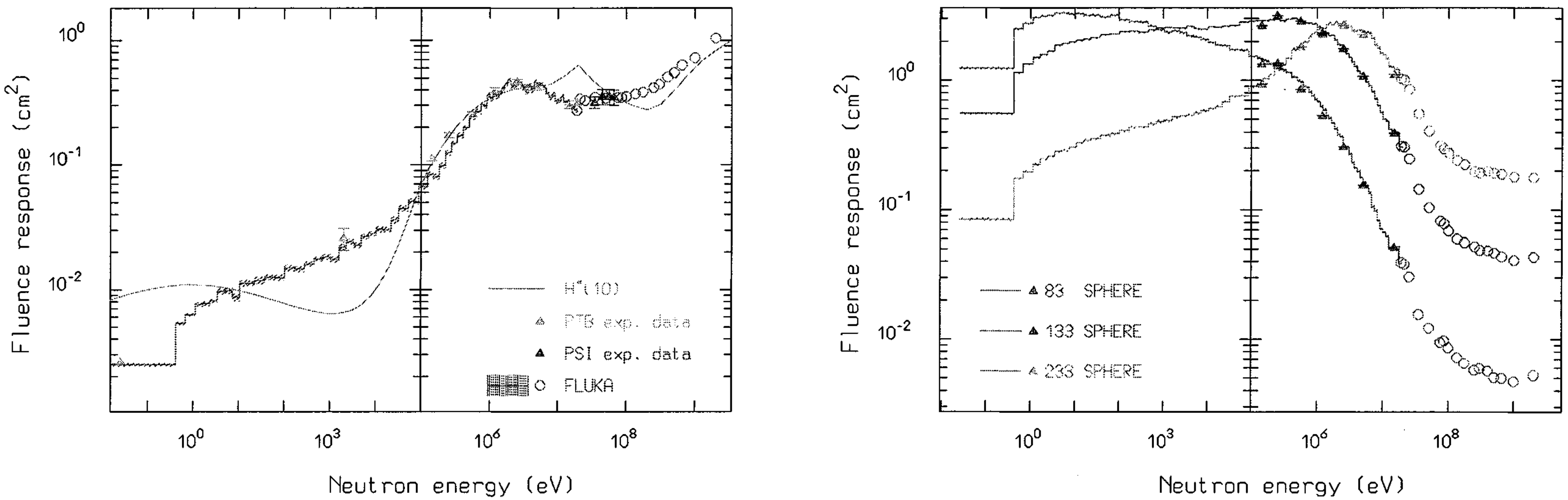

Calibration of the LINUS rem counter (left) and of three Bonner spheres (right) with monoenergetic neutron beams at PTB–Braunschweig and with semi–monoergetic neutron beams at PSI (full symbols), compared with simulations (dashed histos and open circles)

CERF: layout

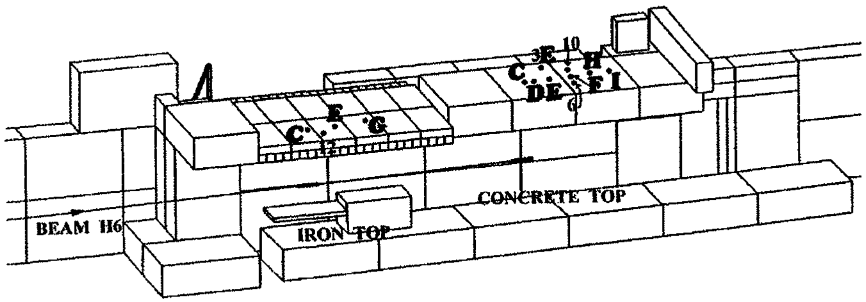

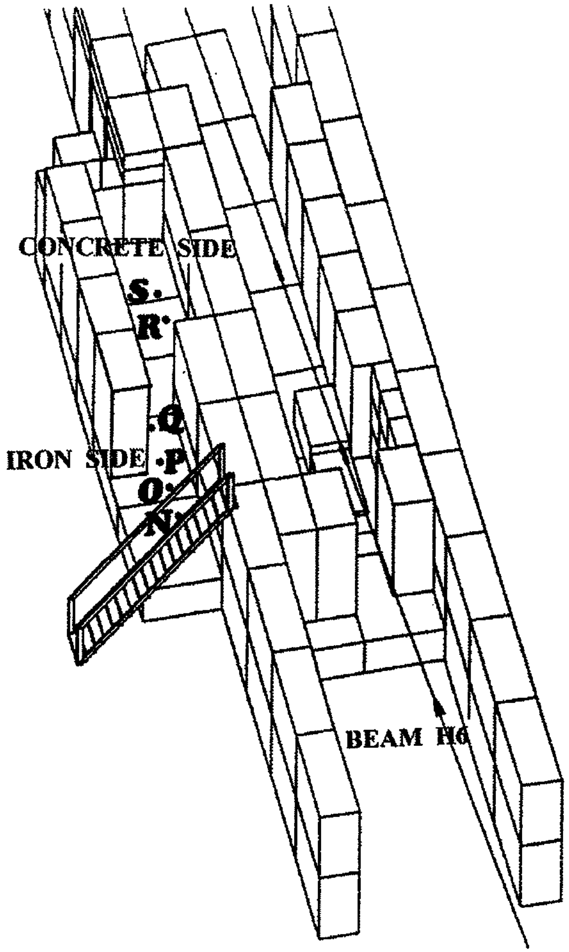

Top (left, one side removed) and side (right, roof removed) views of the CERF facility with the measuring positions.

CERF: some results

	experimental cts/PIC	%	FLUKA cts/PIC	%	experimental cts/PIC	%	FLUKA cts/PIC	%
	CONCRETE TOP "E"				IRON TOP "C"			
LINUS rem counter*	0.364	0.36	0.409	2.2	1.78	0.30	1.68	2.1
SNOOPY rem counter*	0.200	0.59	0.207	3.3	1.83	0.75	1.71	2.0
233 sphere	0.788	0.33	0.899	3.7	9.28	0.28	9.23	2.0
178 sphere	0.989	0.36	1.01	3.4	16.1	0.24	16.9	1.9
133 sphere	1.02	0.30	0.981	3.2	19.2	0.19	21.2	1.9
108 sphere	0.942	0.35	0.883	3.1	17.7	0.20	19.2	1.9
83 sphere	0.704	0.30	0.717	3.1	11.2	0.26	12.1	1.9

Comparison between the FLUKA predictions and the experimental response of the various detectors in stray radiation fields at CERN [9]. The percent statistical uncertainty (%) is indicated.

[9] C.Birattari et al., Rad.Prot.Dos.**76** (1998) 135

Neutron production examples: TARC (PLB458 (1999) 167)

Experiment

Protons from the CERN PS , 2.5 or 3.57 GeV/c

Lead target , 334 ton , 99.99% purity

64 Instrumentation holes, different detectors to measure from thermal to MeV

Simulations: EA MC

Spallation and transport down to 19.6 MeV : FLUKA

Further neutron transport and interactions: new code

Neutron production examples: TARC (PLB458 (1999) 167)

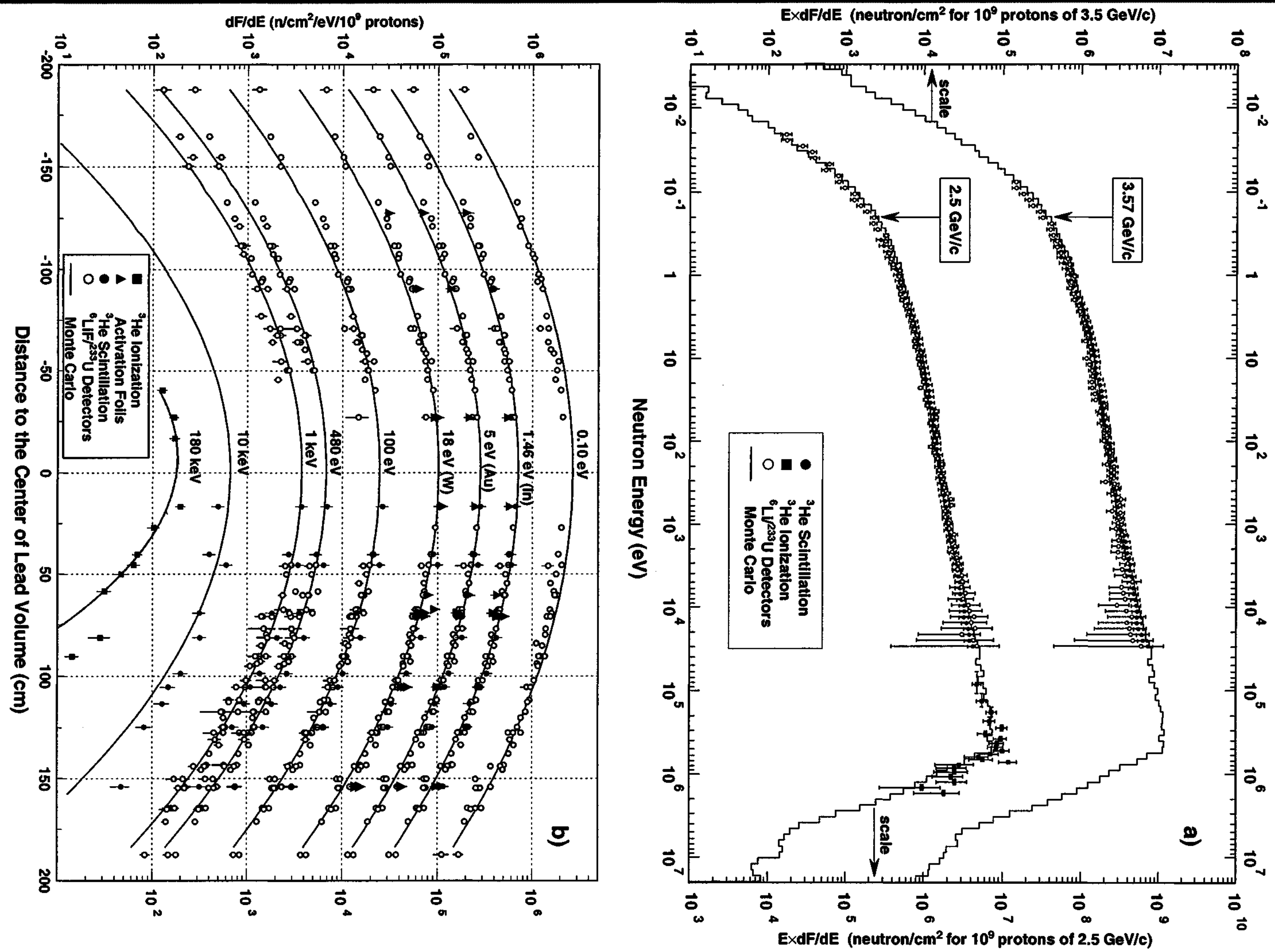

The TIARA neutron propagation experiment

- Source term: neutron spectra generated by 43 and 68 MeV protons on a ^{7}Li target, carefully measured with TOF tecniques
  Quasi-monoenergetic neutrons of $\mathbf{40\ MeV}$ and $\mathbf{65\ MeV}$
- Attenuation of the neutron beam at different depths in concrete and iron shields, both on axis and off-axis (*critical for elastic scattering!!*)
- Emerging neutron spectra measured with liquid scintillator detectors (the high energy component) and Bonner spheres (the low energy component)

H. Nakashima et al. Nucl. Sci. Eng. **124** (1996) and N. Nakao et al. Nucl. Sci. Eng. **124** (1996) 228

The TIARA exp.: FLUKA vs exp. data (concrete on axis)

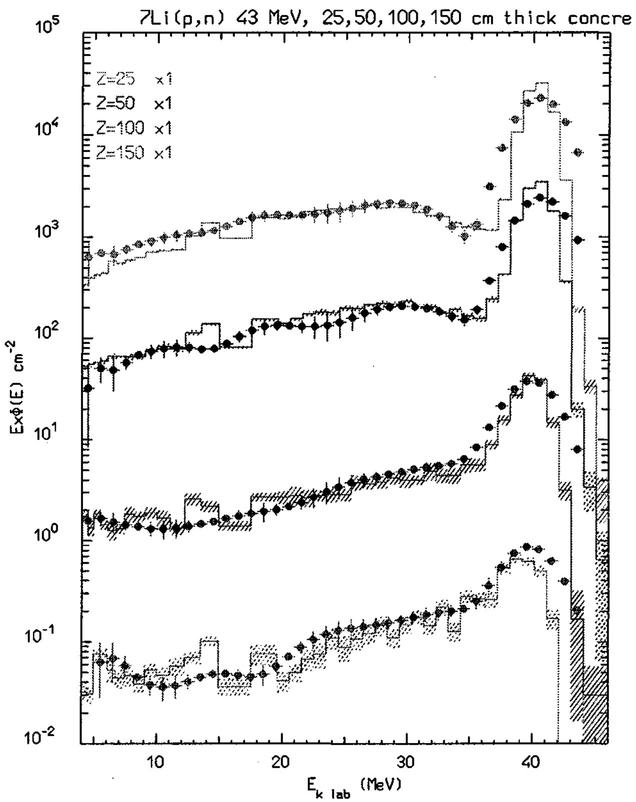

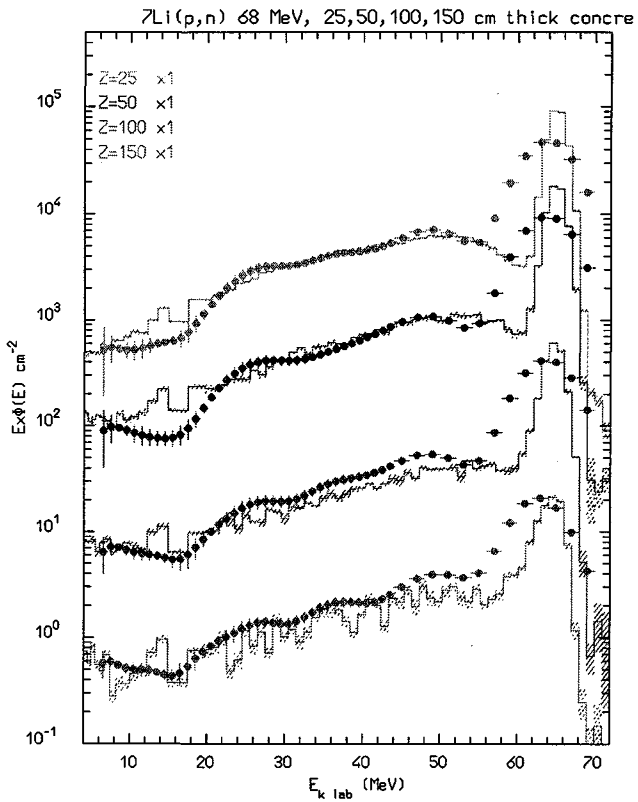

Comparison of simulated (dashed histogram) and measured (symbols) neutron spectra after different concrete thicknesses (from 25 to 150 cm), on axis. The neutrons are generated by ^{7}Li(p,n) at 43 (left) and 68 MeV (right)

The TIARA exp.: FLUKA vs exp. data (iron on axis)

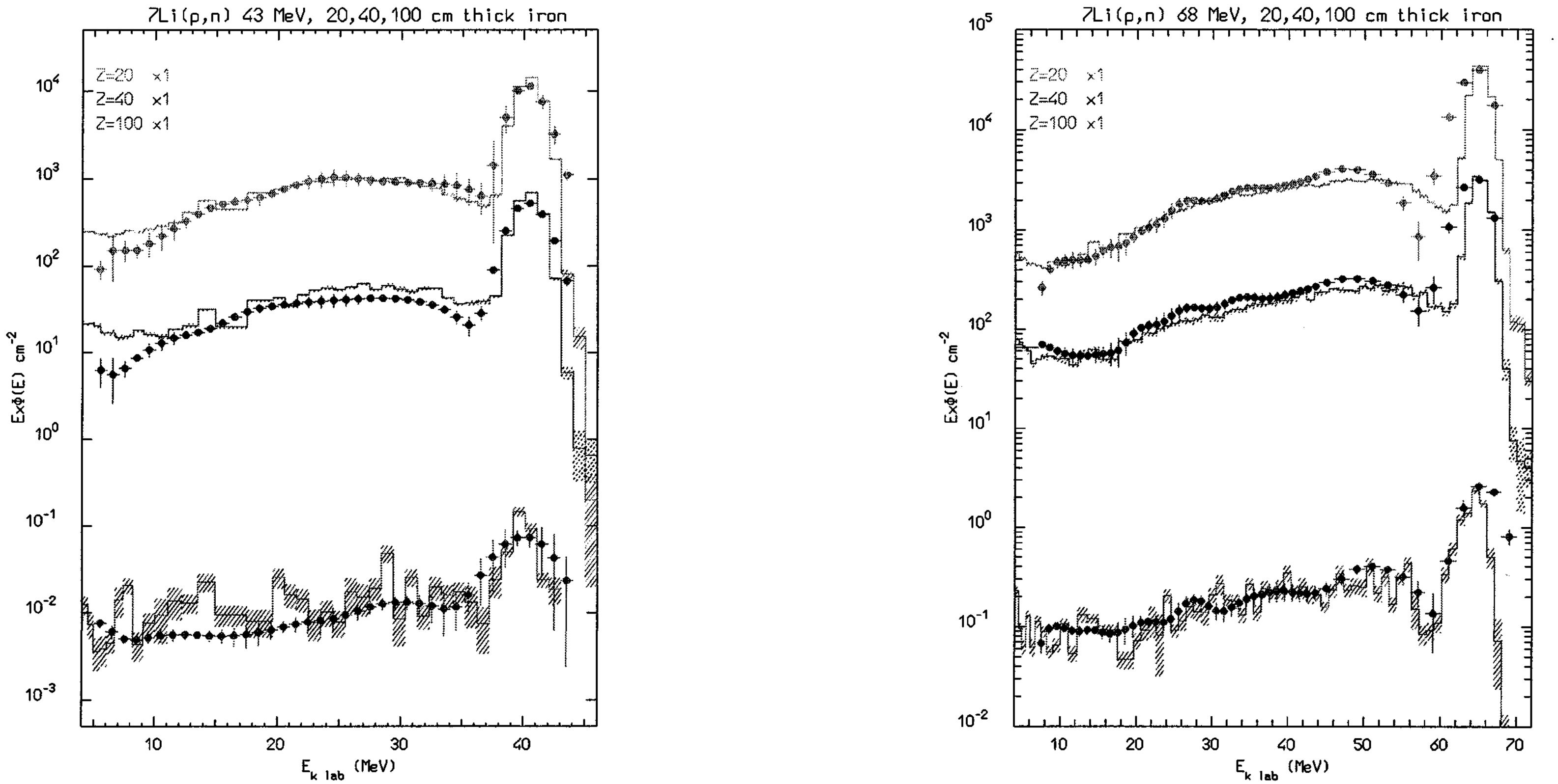

Comparison of simulated (dashed histogram) and measured (symbols) neutron spectra after different iron thicknesses (from 20 to 100 cm), on axis. The neutrons are generated by ^{7}Li(p,n) at 43 (left) and 68 MeV (right)

The TIARA exp.: FLUKA vs exp. data (concrete off axis)

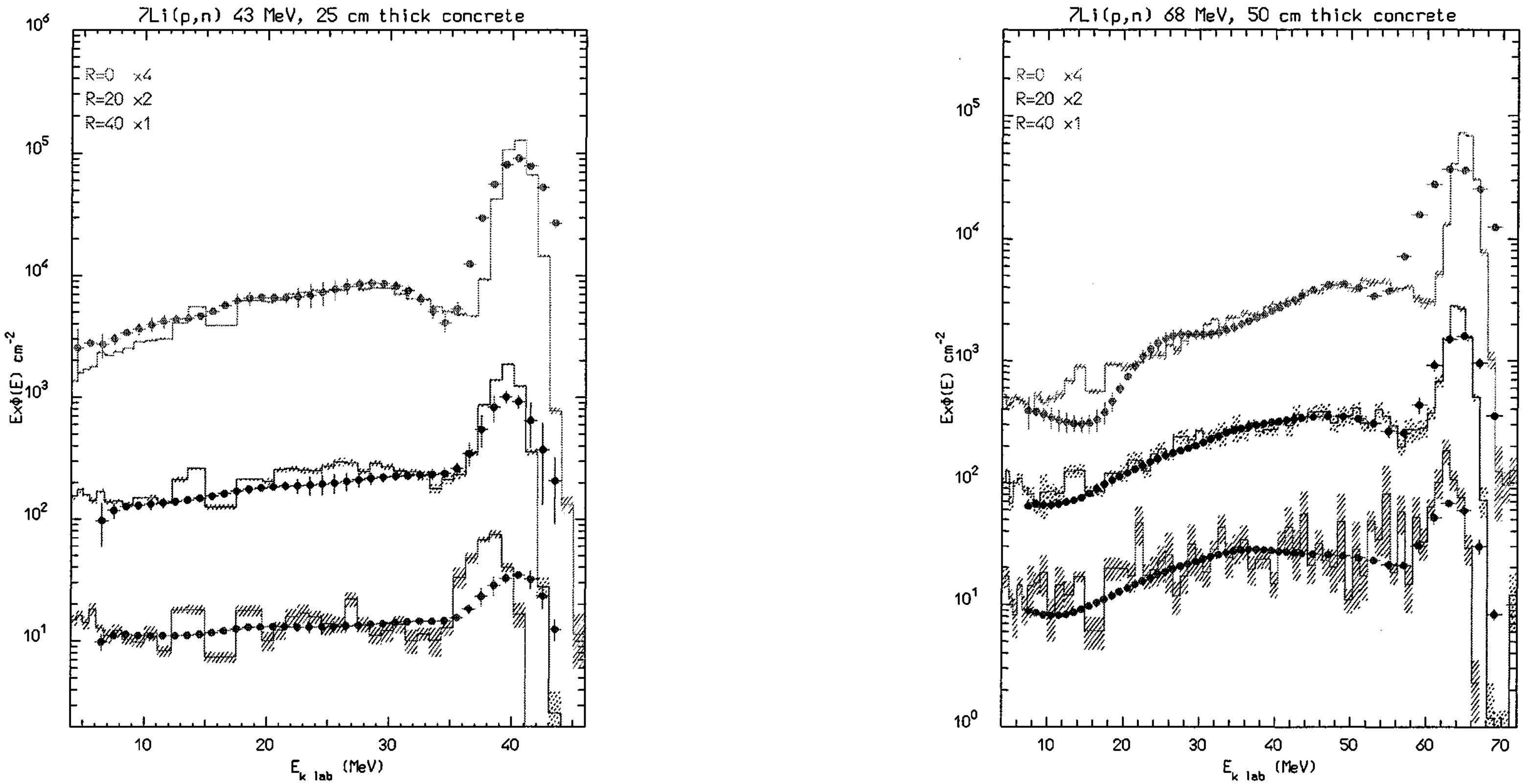

Comparison of simulated (dashed histogram) and measured (symbols) neutron spectra off axis (from 0 to 40 cm) after 25 (left) and 50 cm thick concrete shields. The neutrons are generated by ^{7}Li(p,n) at 43 (left) and 68 MeV (right)

The TIARA exp.: FLUKA vs exp. data (iron off axis)

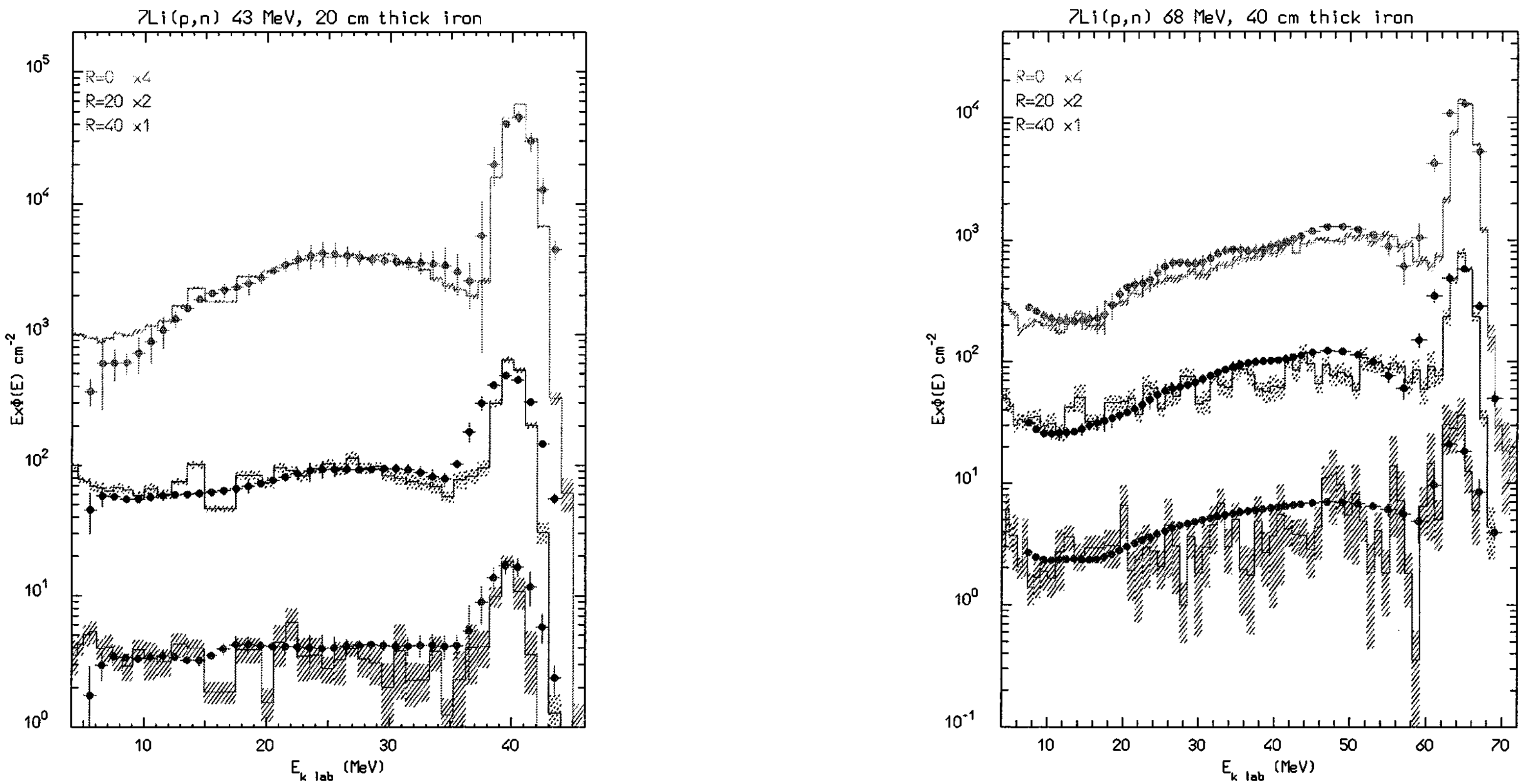

Comparison of simulated (dashed histogram) and measured (symbols) neutron spectra off axis (from 0 to 40 cm) after 20 (left) and 40 cm thick iron shields. The neutrons are generated by ^{7}Li(p,n) at 43 (left) and 68 MeV (right)

Future developments:

- Ion interactions:
  - Consolidation and benchmarking of the interface with DPMJET
  - Extension of the present nuclear models to handle light ions in the intermediate energy range
- A new powerful and user friendly interface through the ROOT system
- Residual activity and dose rates: *Online use of databases for:*
  - *Cooldown* calculations (already implemented offline)
  - γ, β *and* α radiation emission and transport online.
- DPM: add multi-Pomeron exchanges
- PEANUT extension to high energy
- Refinements to evaporation, inclusion of heavy fragment emission
- New low energy neutron library

Different Applications

The FLUKA development, its accuracy and versatility originated to a great deal from the needs of the author experiments, and new applications arise from new code capabilities, with a continuous interplay which is always physics driven. Examples are given below.

- Neutrino physics and Cosmic Ray studies: initiated within ICARUS
  - Neutrino physics: ICARUS, CNGS, NOMAD, CHORUS
  - Cosmic Rays: First 3D ν flux simulation, Bartol, MACRO, Notre-Dame, AMS
- Accelerators and shielding : the very first FLUKA application field
  - Beam-machine interactions: CERN, NLC, LCLS
  - Radiation Protection: CERN, INFN, SLAC, Rossendorf
  - Waste Management and environment: LEP dismantling, SLAC
- Background and radiation damage in experiments: Pioneering work for ATLAS
  - all LHC experiments, NLC

Different Applications

- Dosimetry, radiobiology and therapy :
  - Dose to Commercial Flights: E.U., NASA
  - Dosimetry: INFN, ENEA, GSF, NASA
  - Radiotherapy: Already applied to real situations (Optis at PSI, Clatterbridge)
  - Dose and radiation damage to Space flights: NASA, ASI
- Calorimetry:
  - ATLAS test beams
  - ICARUS
- ADS, spallation sources (FLUKA+EA-MC, C.Rubbia et al.)
  - Energy Amplifier
  - Waste trasmutation with hybrid systems
  - Pivotal experiments on ADS (TARC, FEAT)
  - nTOF